Bioorganic Chemistry 98 (2020) 103720

Contents lists available at ScienceDirect

Bioorganic Chemistry

journal homepage: www.elsevier.com/locate/bioorg

Novel 1*H*-pyrazolo[3,4-*d*]pyrimidin-6-amino derivatives as potent selective Janus kinase 3 (JAK3) inhibitors. Evaluation of their improved effect for the treatment of rheumatoid arthritis

Yuan Yin[a], Cheng-Juan Chen[b], Ru-Nan Yu[a], Lei Shu[a], Zhi-Jian Wang[a], Tian-Tai Zhang[b,*], Da-Yong Zhang[a,*]

[a] School of Science, China Pharmaceutical University, Nanjing, PR China
[b] Institute of Materia Medica, Chinese Academy of Medical Sciences and Peking Union Medical College, Beijing 100050, PR China

ARTICLE INFO

Keywords:
JAK3 inhibitors
Pyrazolo[3
4-*d*]pyrimidin
Rheumatoid arthritis
Autoimmune diseases

ABSTRACT

Selective JAK3 inhibitors have been shown to have a potential benefit in the treatment of autoimmune disorders. Here we report the identification of a series of pyrazolopyrimidine derivatives as potent JAK3 inhibitors that exploit a unique cysteine (Cys909) residue in JAK3. Most of these compounds (**13k**, **13n** and **13 t**), displayed stronger anti-JAK3 kinase activity and selectivity than tofacitinib. Furthermore, the most active inhibitor **13t** (IC_{50} = 0.1 nM), also exhibited favourable selectivity for JAK3 in a panel of 9 kinases which contain the same cysteine. In a series of cytokinestimulated cellular analysis, compound **13 t**, could potently block the JAK3-STAT signaling pathway. Further biological studies, including cellular antiproliferative activity assays and a rat adjuvant-induced arthritis model for in vivo evaluation, also indicated its efficacy and low toxicity in the treatment of rheumatoid arthritis. The results of these experimental explorations suggested that **13t** is a promising lead compound for the development of selective JAK3 inhibitor with therapeutic potential in rheumatoid arthritis.

1. Introduction

Rheumatoid arthritis (RA) is a chronic, systemic inflammatory joint disease, which is characterized by persistent inflammatory synovitis, cartilage and bone lesions, and eventually leads to physical disabilities if not treated properly [1–3]. Proteinases, pro-inflammatory cytokines and chemokines have important function on the multistep pathogenesis of RA, and these proteins can be considered as potential therapeutic targets for RA [2–3]. Among them, the Janus kinases (JAKs) are attractive targets owing to its basic functions and immunosuppressive effects in cytokine signaling network and evidences by JAK inhibitors in clinical use [4]. So far, the use of JAK inhibitors have been a breakthrough for the treatment of autoimmune diseases such as RA, psoriasis and systemic lupus erythematosus (SLE) [5].

Janus kinases (JAKs) are an important family of intracellular protein tyrosine kinases (PTKs) required for signaling through type I/II cytokine receptors. There are four JAK family members, JAK1, JAK2, JAK3, and TYK2 [6–7]. Unlike the rest of JAKs that are widely expressed in many mammalian tissues, JAK3 is expressed primarily in lymphocytes where it associates with type I cytokine receptors featuring a common γ-chain (γc) subunit, and conveys signals from six known cytokines, including IL-2, IL-4, IL-7, IL-9, IL-15, and IL-21, that regulates cell development, division and proliferation in immune system [8–10]. Mutations in either the γ-chain or JAK3 have been identified in humans and mice as a cause of severe combined immunodeficiency disease (SCID), resulting in loss of T and NK cells, abnormal B cell function and hypoplasia of lymphoid tissues with no other defects. [10–11] Given that JAK3 have essential function in immune signaling and JAK3-SCID patients have defects but only limited to immune cells [4–5] Therefore, selective targeting of JAK3 has been identified as a potential mechanism to treat RA and other autoimmune diseases.

Over the past decade, there have been extensive efforts to identify and design novel transformative small-molecule JAK3 inhibitors to address unmet medical needs such as RA, inflammatory bowel disease (IBD) and other autoimmune diseases. Tofacitinib, a first-in-class JAK3 inhibitor, was approved by the U.S. FDA for treatment of adults with moderately to severely active RA in 2012. [10,12] Although Tofacitinib provides a good treatment for RA, it also causes several severe side effects, which are possibly caused by the inhibition of JAK2. Therefore, a selective inhibitor that maintains efficacy, but avoids JAK related adverse events could provide even greater benefit to patients. [12–14]

* Corresponding authors at: School of Science, China Pharmaceutical University, 639 Longmian Avenue, Nanjing, PR China.
E-mail addresses: ttzhang@imm.ac.cn (T.-T. Zhang), cpuzdy@163.com (D.-Y. Zhang).

https://doi.org/10.1016/j.bioorg.2020.103720
Received 19 March 2019; Received in revised form 24 November 2019; Accepted 2 March 2020
Available online 05 March 2020
0045-2068/

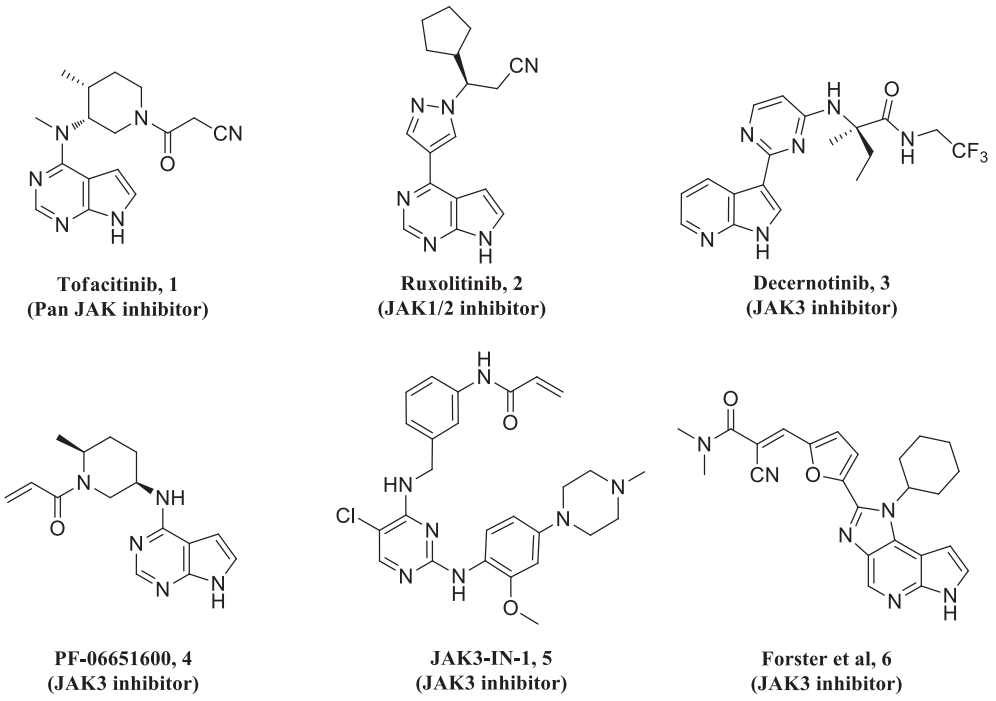

Fig. 1. Chemical structures of representative JAK inhibitors.

The high homology (80–90%) of the JAKs ATP binding pockets has posed a considerable challenge to medicinal chemists seeking to develop highly selective inhibitors as clinical drugs [15–16]. There are few highly selective JAK3 inhibitors in clinical stages to date [17]. Thus, to alleviate the undesirable side effects of JAK1 and JAK2 inhibition, identification of highly selective JAK3 inhibitors would still be in urgent need.

In our efforts to develop a more selective JAK3 inhibitor, we noted that among the JAK family members, JAK3 is unique in having a cysteine residue at the gatekeeper-plus-7 (GK + 7) position [18]. This residue is Cys909 in human JAK3, and it is structurally equivalent to the cysteine residues in the epidermal growth factor receptor (EGFR) and Bruton's tyrosine kinase (BTK). The cysteine residues can be used to confer selectivity by targeting the formation of a covalent interaction [19–21]. Afatinib targets Cys797 in EGFR [19], and ibrutinib targets Cys481 in BTK [20]. Employing this mechanism, several researchers have disclosed their studies on covalent JAK3 inhibitors, such as JAK3-IN-1 [15], PF-06651600 [22], Forster et al. [23] and Smith et al. [24] (Fig. 1). Guided by those achievements and our previous structure-activity relationship (SAR) studies [25,26], we designed and synthesized a series of pyrazolopyrimidines analogues by applying the conformational constraint strategy (Fig. 2), which is an effective method to improve ligand selectivity for a molecular target. Fortunately, the evaluation of these compounds for the inhibition of the JAK3 target provided exciting results, where several molecules appeared to inhibit JAK3 kinase at concentrations of 1.5 nM as well as having excellent JAK kinase selectivity (> 376-fold). More importantly, compound **13t** also exhibits excellent anti-rheumatic effect in the adjuvant-induced arthritis (AIA) model, suggesting that **13t** had the potential to be an efficacious treatment for RA.

2. Results and discussion

2.1. Chemistry

The title molecules **13a-13w** and **14a-14f** were prepared according to the synthesis strategy [27–29], displayed by Schemes 1-3.

The commercially available material 5-hydroxymethyluracil was oxidated using $AgNO_3$-$K_2S_2O_8$ at elevated temperature to yield the 2,4-dihydroxypyrimidine-5-carbaldehyde (**8**). Subsequent $POCl_3$ mediated chlorination of **8** afforded dichloropyrimidine **9**, which was cyclized to provide the pyrazolopyrimidine intermediates **10**. Then, the key

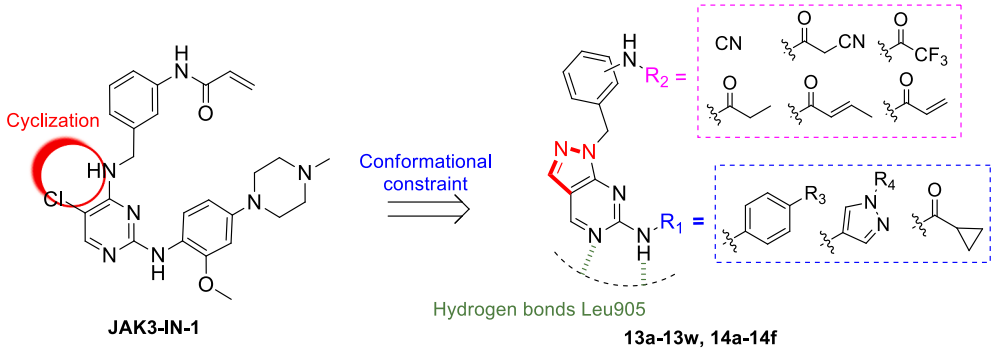

Fig. 2. Designed strategy of the title molecules as JAK3 inhibitor.

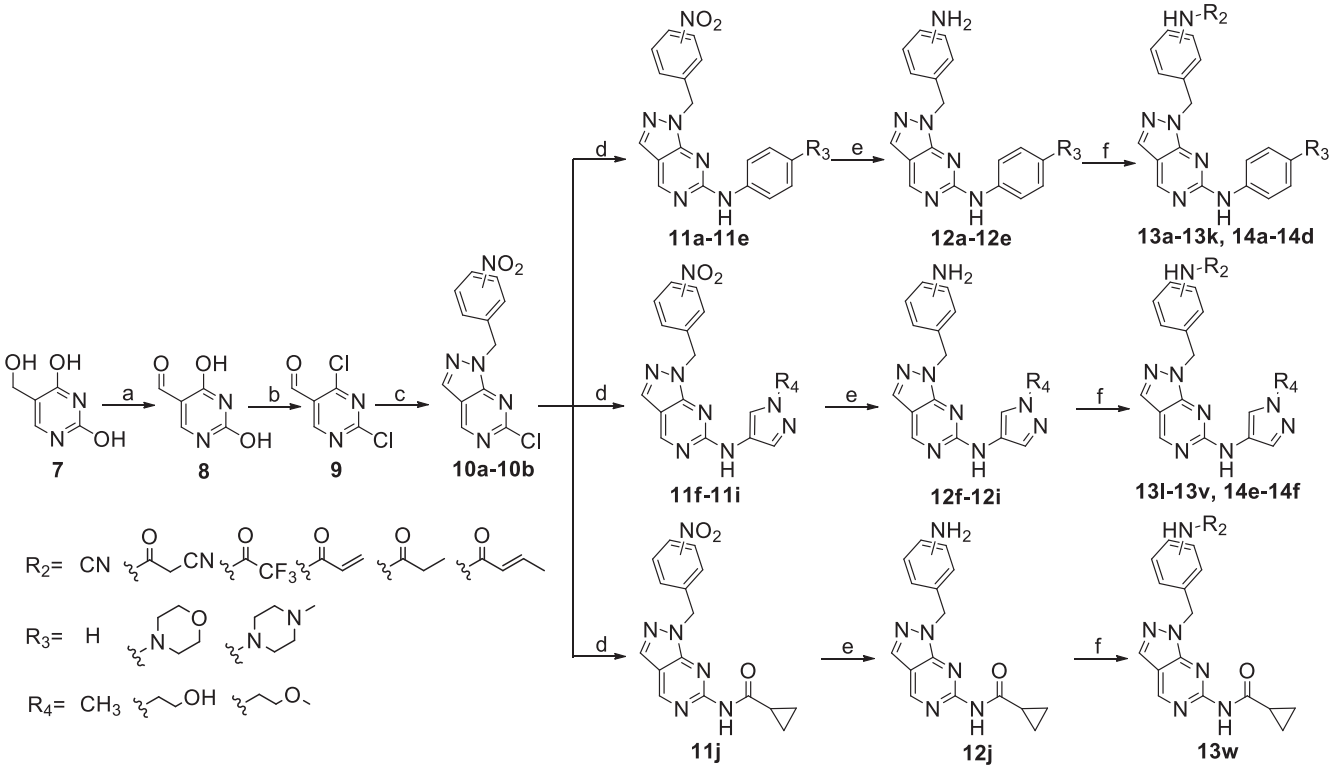

Scheme 1. Synthesis of compounds 13a-13w and 14a-14f. Reagents and conditions: (a) $K_2S_2O_8$, $AgNO_3$, H_2O, 90 °C, 0.5 h, 40 °C, 0.5 h; (b) $POCl_3$, TEA, r.t, 0.5 h, reflux, 3 h; (c) TEA, THF, 0 °C, 0.5 h, r.t., 4 h; (d) TEA, IPA, reflux, 10 h; (e) Pd/C, $N_2H_4{\cdot}H_2O$, EtOH, reflux, 0.5–2 h; (f) Method A: RCOCl, THF, 0 °C, 0.5 h, r.t., 2 h; Method B: BrCN, KOAc, MeOH, 0 °C-r.t., 16 h; Method C: RCOOH, HATU, DIEA, DMF, 0 °C, 0.5 h, r.t., 16 h; Method D: trifluoroacetic anhydride, TEA, THF, 0 °C- r.t., 12 h.

intermediates **11a-11j** were conveniently synthesized by coupling various substituted amines with the pyrazolopyrimidine **10**. Finally, the desired pyrazolopyrimidine derivatives were furnished by reduction of the nitro group followed by acylation with carboxylic acids, acyl chlorides or trifluoroacetic anhydride. The desired cyanide derivatives were conveniently synthesized from **12a to 12j** using cyanogen bromide. The key intermediate amines **17a-17c**, **20a-20c** were prepared by nucleophilic substitution and reduction reactions, as shown in Schemes 2–3.

2.2. Biological activity

2.2.1. In vitro kinase inhibitory activity

To elucidate the structural requirements to achieve potent and selective inhibition of JAK3, we prepared approximately 30 analogues. To approach this optimization in a systematic fashion, this chemotype was divided into two moieties, tail (R_1) and arm (R_2), and each of these moieties were varied sequentially. The anilines tail moiety of **13a** was replaced with different anilines, amindes, or 4-aminopyrazoles, the 1-acrylamidobenzyl arm of **13a** was substituted with functional groups at the anilines, double bond or phenyl ring position. All the newly synthesized compounds were evaluated for their activity against the JAK1-3 enzymes by using the HTRF (Homogenous Time-Resolved Fluorescence) detection technology (Table 1) [30].

Our initial efforts focused on modification of the tail moiety (R_1). We first made compound **13a** which bears an aniline at 6-position to explore the rationality of conformational constraint strategy. To our delight, compared with the positive control JAK3-IN-1 (IC_{50} = 6.3 nM), compound **13a** showed a remarkably improved inhibitory activity and selectivity. On the basis of **13a**, compounds with 4-morpholinylaniline (**13f**) and 4-(4-methylpiperazin-1-yl) aniline (**13k**) tails remarkably inhibited JAK3, with IC_{50} values of 1.4 nM and 0.9 nM, respectively. Furthermore, **13f** and **13k** showed excellent selectivity within the JAK kinases, with 376–2045-fold higher IC_{50} against JAK1 or JAK2. Replacement of the aniline at the 6-position with 1-methyl-1*H*-pyrazol-3-amine group (**13n**) afforded a 20-fold increase in JAK3 inhibitory activity as compared to **13a**. Moreover, **13n** also showed a 7700–30000 fold selectivity window over JAK1 and JAK2. Several analogues elaborated with a 2-substituted ethyl group (**13q-13v**) showed good potency. To our surprise, the most active inhibitor **13t**, with a 2-

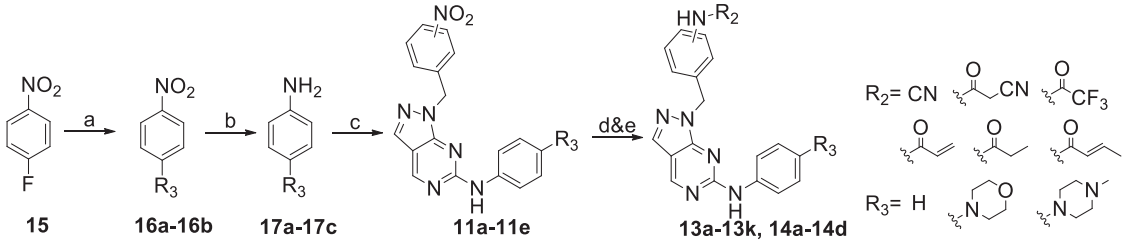

Scheme 2. Synthesis of compounds 17a-17c. Reagents and conditions: (a) K_2CO_3, DMSO, 120 °C, 6 h; (b) Pd/C, $N_2H_4{\cdot}H_2O$, EtOH, reflux, 0.5–2 h; (c) TEA, IPA, reflux, 10 h; (d) Pd/C, $N_2H_4{\cdot}H_2O$, EtOH, reflux, 0.5–2 h; (e) Method A: RCOCl, THF, 0 °C, 0.5 h, r.t., 2 h; Method B: RCOOH, HATU, DIEA, DMF, 0 °C, 0.5 h, r.t., 16 h.; Method C: BrCN, KOAc, MeOH, 0 °C-r.t., 16 h; Method D: TFAA, TEA, THF, 0 °C, 0.5 h, r.t., 12 h.

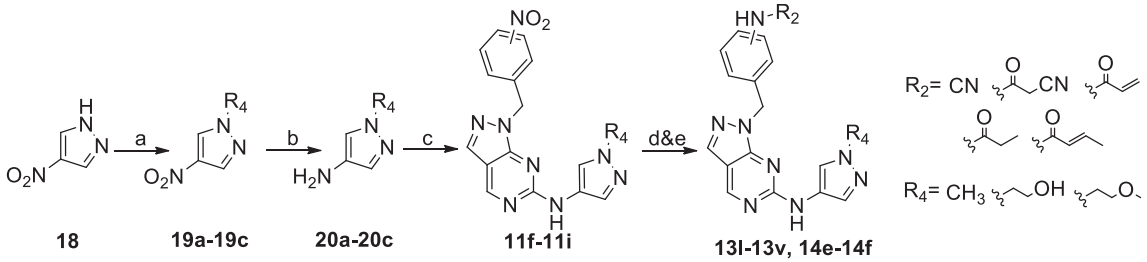

Scheme 3. Synthesis of compounds 20a-20c. Reagents and conditions: (a): K_2CO_3, KI, MeCN, 82 °C, 10 h; (b) Pd/C, H_2, MeOH, r.t., 2 d; (c) TEA, IPA, reflux, 10 h; (d) Pd/C, $N_2H_4{\cdot}H_2O$, EtOH, reflux, 0.5–2 h; (e) Method A: RCOCl, THF, 0 °C, 0.5 h, r.t., 2 h; Method B: RCOOH, HATU, DIEA, DMF, 0 °C, 0.5 h, r.t., 16 h.; Method C: BrCN, KOAc, MeOH, 0 °C-r.t., 16 h.

methoxyethyl, exhibited an IC_{50} of 0.1 nM against JAK3 and over 13000-fold selectivity over other JAKs. Compared with the two representative JAK3 inhibitors JAK3-IN-1 (IC_{50} = 6.3 nM) and tofacitinib (IC_{50} = 1.6 nM), the most potent JAK3 inhibitor **13t** showed a remarkably improved inhibitory activity (16- and 63- fold higher). Replacement of the 2-methoxyethyl with a 1-hydroxyethyl (**13q**) resulted in a decrease in potency (approximately 27-times). Cyclopropanecarboxamide tails resulted in a drastic loss of potency (**13w**). After optimization of the R_1 moiety, the SAR of the arm (R_2) was investigated. Replacing the acrylamide with cyanide (**13r**), cyanoacetamide (**13s**) or propionamide (**13u**) resulted in over 100-fold decrease of potency against JAK3. Installation of a methyl group at the *β*-position of the acrylamide (**13v**) resulted in significant loss of potency and selectivity. Switching the acrylamide from *meta* to *para* on the phenyl ring also decreased JAK3 inhibitory activity and selectivity (**14c-14f**). Overall, the pyrazolopyrimidines with an acrylamide group showed excellent JAK3 inhibitory activity and selectivity, and nearly one half of them (with IC_{50} values of lower than 1.6 nM) displayed stronger activity than JAK3-IN-1 and tofacitinib. Among them, four compounds **13f**, **13k**, **13n** and **13t** (with 376–31020-fold higher IC_{50} against JAK1 or JAK2) possess higher selectivity than JAK3-IN-1 and tofacitinib, and the most active JAK3 inhibitor **13t**, displayed over 76 times higher selectivity than JAK3-IN-1 and tofacitinib. As kinases that share a cysteine at the structurally equivalent position may also be inhibited non-selectively targeted by covalent kinase inhibitors, we further assessed the selectivity of **13t** against 10 protein kinases that contain a cysteine in the equivalent position as that of JAK3, including the TEC family (BTK, TEC, ITK, ETK and RLK), the EGFR family (EGFR, HER2 and HER4) as well as JAK3 and BLK [31]. Compound (**13t**) exhibited excellent selectivity among this panel of kinases, with a high inhibition (99.6%) of JAK3 and a low inhibition of the other kinases, < 17.2% at 0.1 μM (Table 2). These data indicated that **13t** could potently inhibit JAK3, while retaining a high level of kinase selectivity.

2.2.2. Cellular antiproliferative activities

As enzymatic potencies sometimes do not translate into cellular inhibition, we further characterize the selectivity within the JAK family of compounds **13** and **14** in THP-1, TF-1 and HEL cell lines. These cells were selected since IL-4 can induce JAK1 and JAK3 activation in THP-1 cell lines, the GM-CSF induces JAK2 activation in TF-1 cell lines, while HEL is a $JAK2^{V617F}$ positive erythroleukemia cell line. As shown in Table 3, all the compounds tested demonstrated low potency for the TF-1 and HEL cell lines dependent on the JAK2 and JAK2 ^{V617F} signal pathway. Encouragingly, four compounds (**13f**, **13k**, **13n** and **13t**) displayed higher potency and selectivity against the THP-1 cell lines dependent on the JAK1 and JAK3 signal pathway (> 50-fold). Three of them (**13k**, **13n** and **13 t**) displayed higher activity than the positive control tofacitinib (> 1.5-fold). In particular, compound **13t** showed the strongest inhibited proliferation of the THP-1 cell lines with IC_{50} value of 0.43 μM, and over 230-fold selectivity over other cell lines. On the contrary, the compounds of non-acryloyl substituted (**13r**, **13s**) and *para*-substituted (**14c**, **14f**) were the unsuccessful design that showed a lower potency and selectivity index against THP-1 cell lines. To further explore the immunosuppressive effect of these JAK3 inhibitors, some of the target compounds were selected for evaluation of anti-proliferative effects in an IL-2-induced rat *T*-cell model. The results shown in Table 2 indicated that most of these molecules displayed stronger anti-proliferation capability than tofacitinib, with IC_{50} values ranging from 0.66 to 1.83 μM. It seemed that the cellular potency of these compounds against T cell were consistent with their antiproliferation effect in the THP-1 cell line. Molecule **13t** is the most potent JAK3 inhibitor, exhibiting the strongest capacity (IC_{50} = 0.66 μM) for inhibiting rat *T*-cell proliferation. In comparison to tofacitinib (IC_{50} = 1.84 μM), compound **13t** showed approximately 2.8 times higher inhibitory potency against T cells. In summary, these biological evaluations eventually led to the discovery of the promising inhibitor **13t**, which possesses high anti-JAK3 activity. These biological evaluations suggested that the JAK3 inhibitor **13t** has excellent selectivity in cells and can effectively inhibit the proliferation of IL-2-induced rat *T*-cell.

2.2.3. Effects of the inhibitors on JAK activation and downstream signaling

To further determine the selectivity of **13t** for the inhibition of different JAK isotypes within cells, we used a battery of cytokine-stimulated cell-based assays. Cell lines were preincubated with **13t** and treated with cytokines that employ different JAK heterodimeric or JAK3 homodimeric complexes for signalling. All results were measured by western blot and quantified by greyscale intensity levels. To assess JAK1 and JAK3 signalling, we measured IL-4-induced phosphorylation of STAT6 in THP-1 cells, as well as IL-2-induced phosphorylation of STAT5 in NK-92 cells. In these systems, **13t** significantly repressed the phosphorylation of STAT6 and STAT5 in a dose-dependent manner, and complete inhibition was achieved at a concentration of 1 μM (Fig. 3**A, C**). Additionally, we also tested the inhibition of JAK auto-phosphorylation by **13t** in the THP-1 cell lines. As expected, **13t** inhibited p-JAK3 in a dose-dependent manner upon stimulations by IL-6, and showed a weaker degree of inhibition against p-JAK1 (Fig. 3**B**). Compared with a JAK1 obligatory assay (IL-6 phosphorylation of STAT3 in TF-1 cells) (Fig. 3**D**), **13t** showed a very weak ability to inhibit STAT phosphorylation. Similarly, in Prolactin-mediated phosphorylation of STAT5 in 22Rv-1 cells, and in GM-CSF-mediated phosphorylation of STAT5 in TF-1 cells, which requires the activity of JAK2, the IC_{50} values for **13t** could not be determined accurately (> 10 μM) (Fig. 3**E, F**). These data in the enzyme and cell-based assays confirm that **13t** inhibits the JAK3 isoform rather than JAK1 or JAK2.

2.2.4. Rat adjuvant-induced arthritis (AIA) model

To characterize the effect of **13t** for treatment of autoimmune disease, we established an AIA model in rat to assess its anti-arthritic activity. As shown in Fig. 4, we explored whether **13t** could ameliorate the signs and symptoms of experimental arthritis. Rats treated with **13t** had lower arthritis scores than untreated AIA mice ($p < 0.001$ at 50 and 100 mg/ kg, Fig. 4**A**). The efficacy of **13t** at 50 and 100 mg/kg was comparable with that of tofacitinib at 25 mg/kg. The paws from model group rat had a group mean severity of 3.75, while the groups mean

Table 1
SARs of pyrazolopyrimidine derivatives.

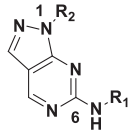

13a-13w, 14a-14f

Compd	R_1	R_2	IC_{50} [a] (nM)			JAK3 S.I.[b]	
			JAK3	JAK1	JAK2	JAK1/JAK3	JAK2/JAK3
13a		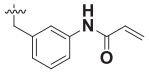	2.6	374	870	144	335
13b		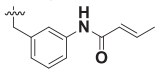	28.9	581	489	20	17
13c	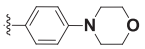	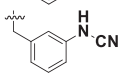	14.1	618	561	44	40
13d	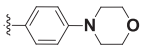	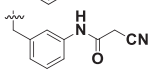	18.4	441	860	24	5
13e	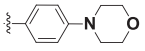	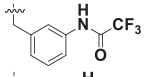	27.9	863	611	31	22
13f	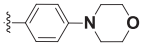	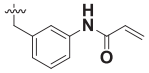	1.4	527	1481	376	1058
13g	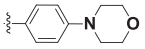	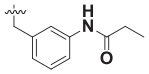	63.1	ND [c]	470	ND	7
13 h	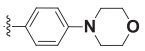	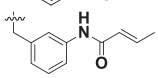	17.3	483	123	28	7
13i	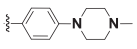	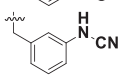	17.3	897	602	52	35
13j	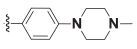	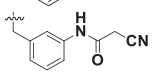	21.4	411	570	19	27
13k	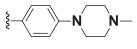	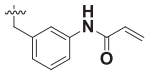	0.9	420	1841	467	2045
13l		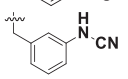	9.4	1051	147	111	16
13m		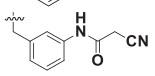	9.7	260	241	27	25
13n		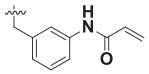	0.13	996	4217	7664	30,121
13o	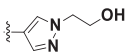	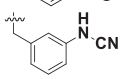	170.3	991	1640	6	10
13p	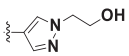	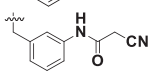	23.7	584	1803	25	76
13q	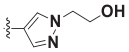	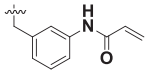	2.73	290	251	106	92
13r	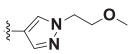	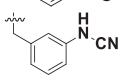	10.1	297	120	29	12
13s	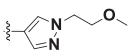	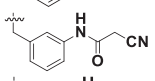	13.5	584	404	43	30
13 t	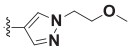		0.10	1301	3102	13,012	31,020
13u			78.0	845	722	11	9

(*continued on next page*)

Table 1 (*continued*)

Compd	R_1	R_2	IC_{50} [a] (nM)			JAK3 S.I.[b]	
			JAK3	JAK1	JAK2	JAK1/JAK3	JAK2/JAK3
13v	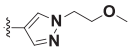	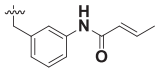	133.3	865	531	7	4
13w		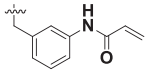	53.2	1852	1905	35	36
14a	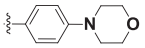	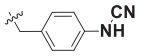	184.2	ND	ND	ND	ND
14b	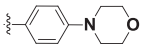	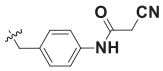	91.4	400	246	4	3]
14c	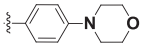	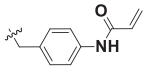	2.2	367	762	167	347
14d	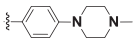	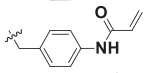	2.4	582	805	243	336
14e		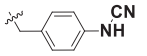	132.0	ND	ND	ND	ND
14f		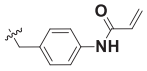	1.9	118	230	62	121
JAK3-IN-1 [d]			6.3	713	1084	113	172
Tofacitinib [e]			1.6	4.3	2.1	3	1

[a] Values are means of three experiments.
[b] S.I.: selectivity index (IC_{50} JAK1/ IC_{50} JAK3 or IC_{50} JAK2/ IC_{50} JAK3).
[c] ND = not determined.
[d] JAK3-IN-1, positive control.
[e] Tofacitinib, positive control.

Table 2
The inhibition % of other kinases that carry similar cysteine residue to Cys909 in JAK3 with 13t.

Compd	% Inhibition (0.1 μM)[a]									
	JAK3	BTK	TEC	ITK	ETK	RLK	EGFR	HER2	HER4	BLK
13t	99.6	11.6	1.72	6.3	1.2	17.2	8.0	2	2.6	9.5

[a] Values represent percent inhibition at 0.1 μM concentration, data are the mean of at least n = 3 independent measurements. Lower numbers indicate stronger binding, where Negative control = DMSO (% inhibition = 100%).

histological severity scores in the **13t** treated rat were 2.33 and 1.67 at dosages of 50 and 100 mg/ kg, respectively. Meanwhile, the histological severity score in the tofacitinib treated group was 2.5 (Fig. 4**B**). Radiographic analysis was conducted on a separate cohort of animals with similar clinical signs of disease treated with model, **13t** or tofacitinib (Fig. 4**C**). Compared with naive healthy rats (Control groulp), ankles from model-treated mice exhibited massive joint destruction. Consistent with the observed histologic effects, orally administered **13t** (50 and 100 mg/kg) improved and restored the normal architecture and appearance to the ankle and tarsals in a dose-dependent manner. Analysis of the major organs and blood indicated no significant side effects of the treatment (Supplementary Table S1 and S2). Additionally, the body weight also showed no decrease during treatment with **13t** (Supplementary Fig. S1). These results suggested the **13t** exhibited a better treatment capability than tofacitinib in arthritis by relieving pathological processes. But, **13t** and tofacitinib (50 mg/kg) were not effective against the acute Dextran Sulphate Sodium (DSS) colitis models (Supplementary Fig. S2).

Table 3
Cellular inhibitory activities for compounds 13 and 14.

Compd	Cellular inhibitory activity (IC_{50} [a], μM)			T cell proliferation IC_{50}[b] (μM)
	THP-1(JAK1/3)	TF-1(JAK2)	HEL($JAK2^{V617F}$)	
13f	1.60 ± 0.42	81.15 ± 22.70	> 100	1.44 ± 0.44
13k	1.07 ± 0.67	> 100	> 100	1.83 ± 0.09
13n	0.56 ± 0.24	> 100	ND [d]	0.85 ± 0.16
13r	26.21 ± 6.69	49.16 ± 6.45	> 100	8.15 ± 2.09
13s	51.10 ± 14.43	24.56 ± 4.24	> 100	10.23 ± 1.63
13 t	0.43 ± 0.15	> 100	> 100	0.66 ± 0.09
14c	6.42 ± 2.88	> 100	> 100	12.63 ± 3.88
14f	9.37 ± 1.98	> 100	> 100	5.75 ± 0.99
Tofacitinib [c]	1.57 ± 0.68	3.13 ± 0.68	7.27 ± 1.25	1.84 ± 0.28

[a] Values are means of three experiments.
[b] Inhibitory effect on IL-2-stimulated T cell proliferation using rat spleen cells (n = 3).
[c] Tofacitinib, positive control.
[d] ND = not determined.

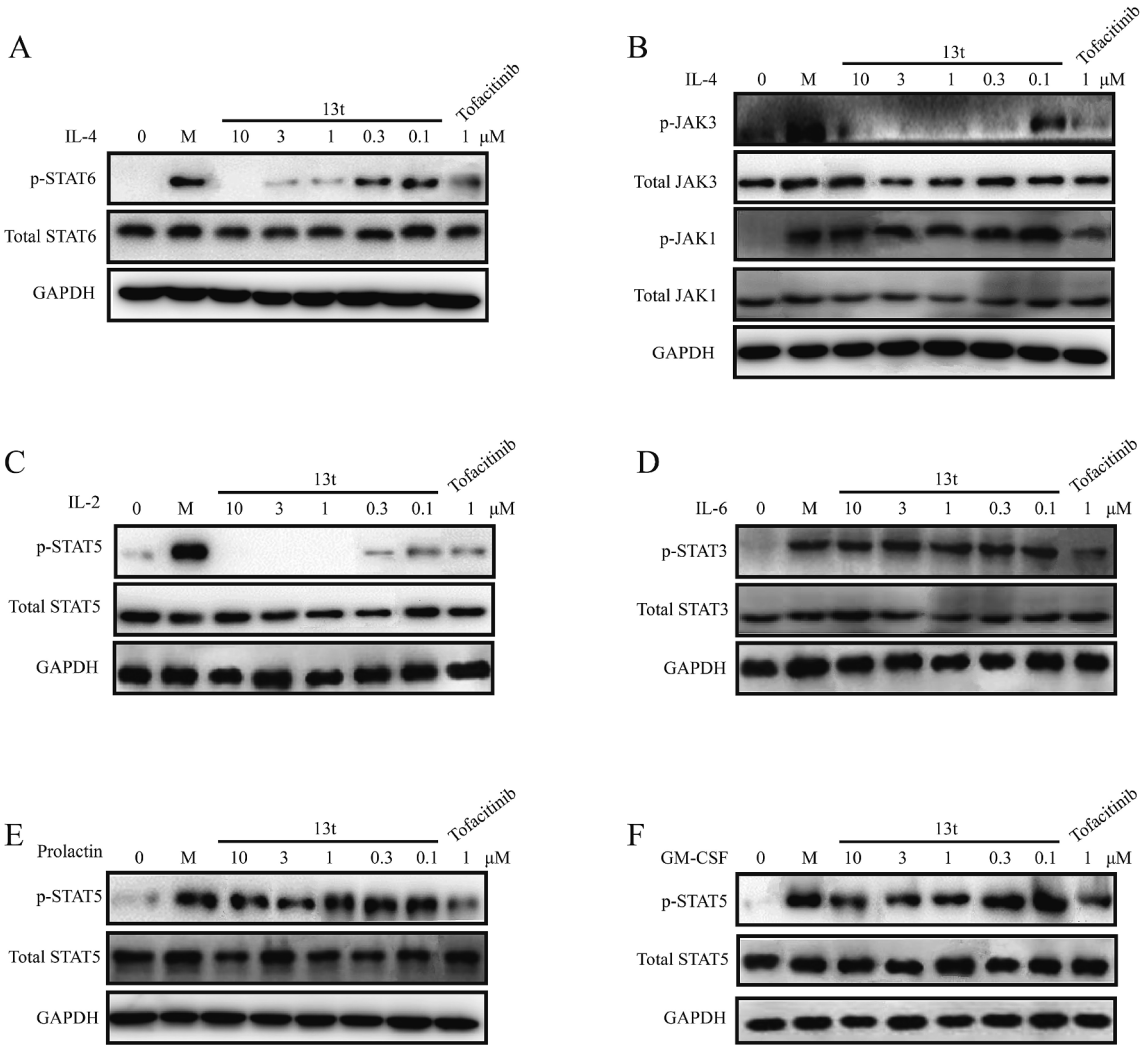

Fig. 3. Identification of **13t** as a highly selective JAK3 inhibitor. Cells were pretreated with **13t** for 1 h, followed by treatment with IL-4, IL-2, IL-6, Prolactin or GM-CSF for an additional 20 to 60 min. Cells were lysed with sample buffer, and the lysates were analysed using immunoblotting. **A**: Western blot analysis of STAT6 phosphorylation after treatment with **13t** in THP-1 cell lines. **B**: Western blot analysis of JAK1 and JAK3 phosphorylation after treatment with **13t** in THP-1 cell lines. **C**: Western blot analysis of STAT5 phosphorylation after treatment with **13t** in NK-92 cell lines. **D**: Western blot analysis of STAT3 phosphorylation after treatment with **13t** in TF-1 cell lines. **E**: Western blot analysis of STAT5 phosphorylation after treatment with **13t** in 22Rv-1 cell lines. **F**: Western blot analysis of STAT5 phosphorylation after treatment with **13t** in TF-1 cell lines.

2.3. Molecular modelling analysis

Three inhibitors, including **13t** (the most active), **13f** (the moderately active), and **13w** (the least active) were docked into the ATP binding pocket of JAK3 (PDB: 4Z16) to investgate the putative interaction mechanism of the pyrazolopyrimidines with the JAK3 enzyme, respectively. The program Discovery Studio 3.0 with its default parameters was used. For comparison, the lead compound JAK3-IN-1 was also analyzed using the same procedure (Fig. 5**A**).

As shown in Fig. 5**A and B**, both inhibitors JAK3-IN-1 and **13t** have tightly contact with JAK3 through several important binding forces, including: (1) The 1*H*-pyrazolo[3,4-*d*]pyrimidin-6-amino moiety of inhibitors makes a bidentate hydrogen bonds with Leu905 in the hinge region; (2) A covalent bond between the acryl amide and the amino acid Cys909. The major difference in JAK3 binding models is that there are a π-π interaction produced by the pyrimidine core of **13t** with the amino acid Tyr904 and two σ-π interactions between the pyrazole group of **13t** with the amino acids Leu828 and Gly908. Presumably, these interactions enhance the activity of **13t** against JAK3. Similarly, the moderately active inhibitor **13f** also retained all these important interaction forces (Fig. 5**C**). Thus, it only has nearly 9 times lower inhibitory potency than inhibitor **13t**. Conversely, the less potent inhibitor **13w** also retained the covalent bond, π-π contacts and a hydrogen bond remained (Fig. 5**D**). However, the cyclopropanecarboxamide functional group at the C-6 position moved far away from Leu905, eventually resulting in the loss of a strong hydrogen bond and twoσ-π interactions. These docking observations reasonably explain the activity data.

3. Conclusion

Inhibiting the activation of JAK3 is a strategy to combat autoimmune diseases. In this study, a number of potent and selective covalent JAK3 inhibitors for the treatment of RA were identified and evaluated. Most of these compounds displayed strong potency to block activity of JAK3 kinase, with IC_{50} values of < 10 nM. In addition, three compounds (**13k**, **13n** and **13 t**) remarkably inhibited the activity of JAK3 at concentrations lower than 1 nM and showed excellent selectivity within the JAK kinases, with 470–31000-fold higher IC_{50}s against JAK1 or JAK2. Further, the most promising JAK3 kinase inhibitor **13t** (IC_{50} = 0.1 nM), displayed high selectivity over other kinases (BTK, TEC, ITK, ETK, RLK, EGFR, HER2, HER4 and BLK) that bear

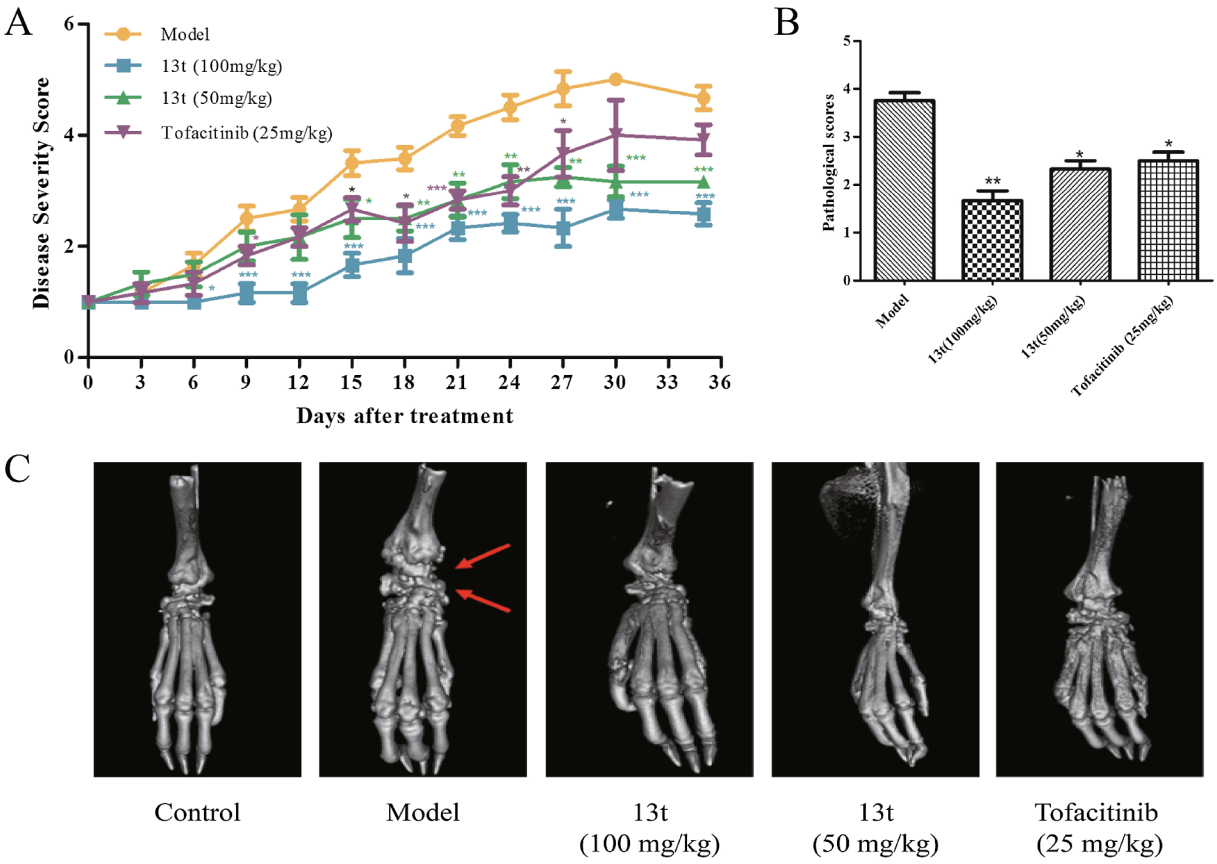

Fig. 4. 13t is efficacious in treating an adjuvant-induced arthritis model. **A**: Clinical scores of AIA rat after treatment with model, Tofacitinib (25 mg/kg), and **13t** (50 mg/kg or 100 mg/kg). Clinical scores were measured three days per time. *p < 0.05, **p < 0.01 and ***p < 0.001 versus model control. **B**: Pathological scores of the joint sections. Bars represent the mean ± S.E.M. (n = 6). *p < 0.05 and **p < 0.01 versus model. **C**: Micro-CT imaging of representative ankles from similarly treated animals showed clear evidence that **13t** normalized the joint architecture and prevented bone destruction (red arrows). (For interpretation of the references to colour in this figure legend, the reader is referred to the web version of this article.)

a similar cysteine residue at the same positions. In cell growth inhibition assays, **13t** showed higher inhibitory activity towards IL-4 dependent THP-1 cell lines (IC_{50} = 0.43 μM) than GM-CSF dependent TF-1 cell lines, and was less toxic to $JAK2^{V617F}$ bearing HEL cells. Furthermore, the cytokine-stimulated cell-based assays and a rat AIA model for in vivo evaluation also indicated **13t** efficiency and low toxicity for the treatment of RA. Overall, these newly discovered selective covalent JAK3 inhibitors are of great enough value to warrant further investigation as potential agents for the treatment of RA and other immune-related diseases.

4. Experimental

4.1. Chemistry

^{1}H NMR and ^{13}C NMR spectra were recorded with a Bruker 300 MHz NMR spectrometer and referenced to deuterium dimethyl sulfoxide (DMSO-d_6) or $CDCl_3$. MS spectra was obtained on an Agilent 6120 quadrupole LC/MS (ESI). HR-ESI-MS was run on an Agilent Q-TOF mass spectrometer. All reagents and solvents were purchased from commercial sources and used as obtained. The solvents used were all AR grade and were redistilled under positive pressure of dry nitrogen atmosphere in the presence of proper desiccant when necessary. Silica gel (200–300 mesh, Qingdao city, China) was used for column chromatography. The progress of the reactions was monitored by analytical thin-layer chromatography (TLC) on HSGF254 precoated silica gel plates.

4.1.1. 2,4-Dihydroxypyrimidine-5-carbaldehyde (8)

Hydroxymethyluracil (14.2 g, 100.0 mmol) was dissolved in H_2O (350 mL)by heating to approximately 90 °C. The solution was then cooled to 45 °C, $K_2S_2O_8$ (40.5 g, 150.0 mmol) and $AgNO_3$ (0.5 g, 3.0 mmol) were added, the product began to slowly precipitate. The reaction was stirred for a further 20 min at 40 °C and then cooled to room temperature over 15 min while stirring was continued. The suspension was then placed at 4 °C, the off-white crystals were collected by filtration, and rinsed with 50 mL of cold water. Yield: 85% (11.9 g, 85.0 mmol). MS (ESI) *m/z*: 141.2 $[M+H]^+$.

4.1.2. 2,4-Dichloropyrimidine-5-carbaldehyde (9)

The intermediate **8** (14.0 g, 100.0 mmol) was slurried in $POCl_3$ (46.0 g, 300.0 mmol). The slurry was warmed to 30 °C and Et_3N (25.3 g, 250.0 mmol) was added dropwise over 30 min, maintaining the temperature at 35–45 °C using an ice-water bath. The slurry was stirred for 0.5 h and then heated to reflux for 3 h. The reaction was cooled to 15 °C and transferred over 3 h into a mixture of H_2O (200 mL). The water layer was extracted with DCM (3 × 80 mL). The organic layers were then washed with water followed by brine. The organic layers were dried over anhydrous sodium sulfate, filtered, and concentrated to provide the crude product, which was purified by silica gel column chromatography (eluting with 0–50% DCM in petroleum ether) to afford a yellow solid. Yield 69% (12.1 g, 68.7 mmol).^{1}H NMR (300 MHz, $CDCl_3$) δ 10.46 (s, 1H), 9.40 (s, 1H).

4.1.3. 6-Chloro-1-(3-nitrobenzyl)-1H-pyrazolo[3,4-d]pyrimidine (10a)

The mixture of **9** (8.8 g, 50.0 mmol) and Et_3N (15.2 g, 150.0 mmol) in THF (150 mL) was stirred at 0 °C for 10 min under argon. To the

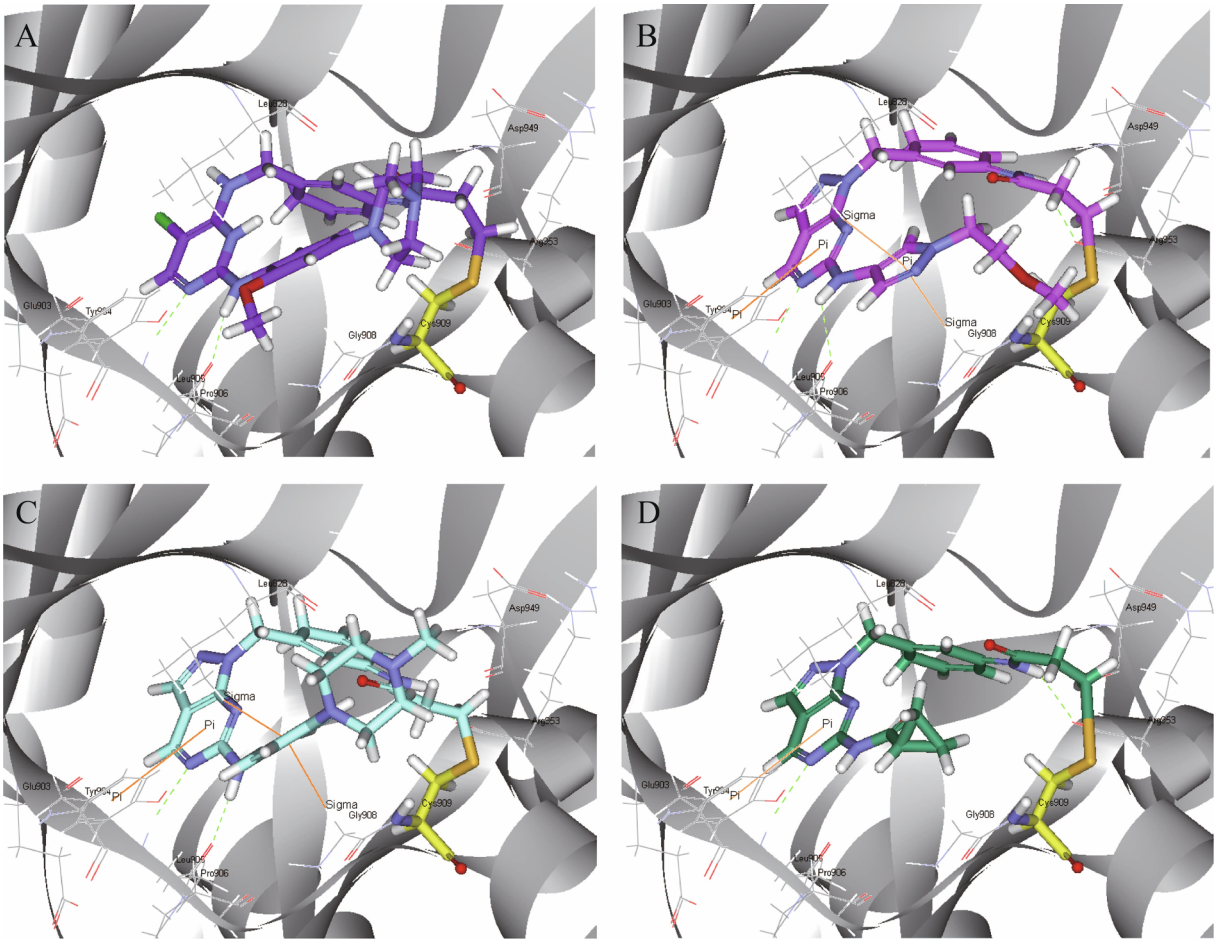

Fig. 5. Proposed binding models of the typical inhibitors with JAK3 enzyme (PDB code: 4Z16). A: JAK3-IN-1, **B**: inhibitor **13t**, **C**: inhibitor **13f**, **D**: inhibitor **13w**.

solution was added 3-nitrobenzylhydrazine dihydrochloride (11.2 g, 55.0 mmol) and then warm to r.t. and stirred for 4 h. The solvent was removed in vacuo, and the residue was partitioned between CH_2Cl_2 (50 mL) and H_2O (100 mL). The layers were separated, and the aqueous layer was extracted with CH_2Cl_2 (2 × 50 mL). The combined organic layers were dried over anhydrous sodium sulfate, filtered, and concentrated to provide the crude product, which was purified by silica gel column chromatography (eluting with 0–10% MeOH in DCM) to provide **10a**, white solid, yield 62% (9.0 g, 31.1 mmol). ^{1}H NMR (300 MHz, $CDCl_3$) δ 8.93 (s, 1H), 8.25 (m, 1H), 8.18 (m, 1H), 8.07 (s, 1H), 7.71 (d, J = 9 Hz, 1H), 7.53 (t, J = 9 Hz, 1H), 5.71 (s, 2H); MS (ESI) m/z: 290.1 $[M+H]^+$.

*4.1.4. 6-Chloro-1-(4-nitrobenzyl)-1H-pyrazolo[3,4-d]pyrimidine (**10b**)*

Compound **9** (8.8 g, 50.0 mmol) and 4-nitrobenzylhydrazine dihydrochloride (11.17 g, 55.00 mmol) was reacted using a procedure similar to the synthesis of **10a**, affording compound **10b**, white solid, yield 56% (8.1 g, 28.0 mmol). ^{1}H NMR (300 MHz, $CDCl_3$) δ 9.06 (s, 1H), 8.19 (s, 1H), 8.18 (d, J = 9 Hz, 2H), 7.50 (d, J = 9 Hz, 2H), 5.72 (s, 2H); MS (ESI) m/z: 290.1 $[M+H]^+$.

General procedure for the synthesis of 11a-11j

A mixture of 6-chloro-1*H*-pyrazolo[3,4-*d*]pyrimidine derivative **10a** or **10b** (25.0 mmol) of each and the appropriate amino derivatives (27.5 mmol) in IPA (300 mL) containing DIEA (62.5 mmol) was heated under reflux for 10 h. The mixture was then placed at 4 °C, the solids were collected by filtration, and rinsed with 50 mL of cold IPA to give compounds.

*4.1.5. 1-(3-Nitrobenzyl)-N-phenyl-1H-pyrazolo[3,4-d]pyrimidin-6-amine (**11a**)*

Compound **10a** (7.2 g, 25.0 mmol) and aniline (2.6 g, 27.5 mmol) were reacted using the general procedure to the synthesis of **11a** as a yellow solid, yield 92%, (8.0 g, 23.0 mmol). ^{1}H NMR (300 MHz, DMSO-d_6) δ 9.06 (s, 1H), 8.27 (m, 1H), 8.20 (m, 1H), 8.07 (s, 1H), 7.72 (d, J = 9 Hz, 1H), 7.62–7.59 (m, 2H), 7.53 (t, J = 9 Hz, 1H), 7.32–7.26 (m, 3H), 5.72 (s, 2H); MS (ESI) m/z: 347.2 $[M+H]^+$.

*4.1.6. N-(4-Morpholinophenyl)-1-(3-nitrobenzyl)-1H-pyrazolo[3,4-d] pyrimidin-6 -amine (**11b**)*

Compound **10a** (7.2 g, 25.0 mmol) and **17b** (4.9 g, 27.5 mmol) were reacted using the general procedure to the synthesis of **11b** as a yellow solid, yield 87%, (9.4 g, 21.7 mmol). ^{1}H NMR (300 MHz, DMSO-d_6) δ 9.05 (s, 1H), 8.20 (m, 1H), 8.16 (m, 1H), 8.05 (s, 1H), 7.75 (d, J = 9 Hz, 1H), 7.72–7.70 (m, 2H), 7.53 (t, J = 9 Hz, 1H), 7.48–7.45 (m, 2H), 5.70 (s, 2H), 4.05 (m, 4H), 3.50 (m, 4H); MS (ESI) m/z: 432.2 $[M+H]^+$.

*4.1.7. N-(4-(4-Methylpiperazin-1-yl)phenyl)-1-(3-nitrobenzyl)-1H-pyrazolo[3,4-d] pyrimidin-6-amine (**11c**)*

Compound **10a** (7.2 g, 25.0 mmol) and **17c** (5.3 g, 27.5 mmol) were reacted using the general procedure to the synthesis of **11c** as a yellow solid, yield 80%, (8.9 g, 20.0 mmol). ^{1}H NMR (300 MHz, DMSO-d_6) δ 9.04 (s, 1H), 8.17 (m, 1H), 8.16 (m, 1H), 8.03 (s, 1H), 7.77 (d, J = 9 Hz, 1H), 7.70–7.67 (m, 2H), 7.53 (t, J = 9 Hz, 1H), 7.46–7.43 (m, 2H), 5.71 (s, 2H), 3.56 (m, 4H), 3.16 (m, 4H), 2.78 (s, 3H); MS (ESI) m/z: 445.2 $[M+H]^+$.

*4.1.8. N-(4-Morpholinophenyl)-1-(4-nitrobenzyl)-1H-pyrazolo[3,4-d] pyrimidin-6 -amine (**11d**)*

Compound **10b** (7.2 g, 25.0 mmol) and **17b** (4.9 g, 27.5 mmol) were reacted using the general procedure to the synthesis of **11d** as a yellow solid, yield 89%, (9.6 g, 22.2 mmol) (9.59 g, 89%). ^{1}H NMR (300 MHz, DMSO-d_6) δ 9.06 (s, 1H), 8.17 (d, J = 9 Hz, 2H), 8.13 (s, 1H), 7.72–7.70 (m, 2H), 7.53 (d, J = 9 Hz, 2H), 7.47–7.44 (m, 2H), 5.72 (s, 2H), 4.04 (m, 4H), 3.49 (m, 4H); MS (ESI) m/z: 432.2 $[M+H]^+$.

*4.1.9. N-(4-(4-Methylpiperazin-1-yl)phenyl)-1-(4-nitrobenzyl)-1H-pyrazolo[3,4-d] pyrimidin-6-amine (**11e**)*

Compound **10b** (7.2 g, 25.0 mmol) and **17c** (5.3 g, 27.5 mmol) were reacted using the general procedure to the synthesis of **11e** as a yellow solid, yield 83%, (9.2 g, 20.7 mmol). ^{1}H NMR (300 MHz, DMSO-d_6) δ 9.06 (s, 1H), 8.15 (d, J = 9 Hz, 2H), 8.10 (s, 1H), 7.72–7.69 (m, 2H), 7.53 (d, J = 9 Hz, 2H), 7.47–7.43 (m, 2H), 5.70 (s, 2H), 3.50 (m, 4H), 3.11 (m, 4H), 2.75 (s, 3H); MS (ESI) m/z: 445.2 $[M+H]^+$.

*4.1.10. N-(1-Methyl-1H-pyrazol-4-yl)-1-(3-nitrobenzyl)-1H-pyrazolo[3,4-d]pyrimidin- 6-amine (**11f**)*

Compound **10a** (7.2 g, 25.0 mmol) and **20a** (2.7 g, 27.5 mmol) were reacted using the general procedure to the synthesis of **11f** as a yellow solid, yield 89%, (7.8 g, 22.3 mmol). ^{1}H NMR (300 MHz, DMSO-d_6) δ 9.01 (s, 1H), 8.25 (m, 1H), 8.18 (m, 1H), 8.07 (s, 1H), 8.03 (s, 1H), 7.70 (d, J = 9 Hz, 1H), 7.53 (t, J = 9 Hz, 1H), 7.49 (s, 1H), 5.70 (s, 2H), 3.81 (s, 3H); MS (ESI) m/z: 351.2 $[M+H]^+$.

*4.1.11. 2-(4-((1-(3-Nitrobenzyl)-1H-pyrazolo[3,4-d]pyrimidin-6-yl) amino)-1H-pyrazol −1-yl)ethanol (**11 g**)*

Compound **10a** (7.2 g, 25.0 mmol) and **20b** (3.5 g, 27.5 mmol) were reacted using the general procedure to the synthesis of **11 g** as a yellow solid, yield 80%, (7.6 g, 20.0 mmol). ^{1}H NMR (300 MHz, DMSO-d_6) δ 9.05 (s, 1H), 8.22 (m, 1H), 8.15 (m, 1H), 8.06 (s, 1H), 8.02 (s, 1H), 7.70 (d, J = 9 Hz, 1H), 7.55 (t, J = 9 Hz, 1H), 7.50 (s, 1H), 5.74 (s, 2H), 4.17 (t, J = 6 Hz, 2H), 3.78 (t, J = 6 Hz, 2H); MS (ESI) m/z: 381.2 $[M+H]^+$.

*4.1.12. N-(1-(2-Methoxyethyl)-1H-pyrazol-4-yl)-1-(3-nitrobenzyl)-1H-pyrazolo[3,4-d] pyrimidin-6-amine (**11 h**)*

Compound **10a** (7.2 g, 25.0 mmol) and **20c** (3.9 g, 27.5 mmol) were reacted using the general procedure to the synthesis of **11 h** as a yellow solid, yield 92%, (9.1 g, 23.0 mmol). ^{1}H NMR (300 MHz, DMSO-d_6) δ 9.05 (s, 1H), 8.20 (m, 1H), 8.15 (m, 1H), 8.09 (s, 1H), 8.03 (s, 1H), 7.71 (d, J = 9 Hz, 1H), 7.52 (t, J = 9 Hz, 1H), 7.57 (s, 1H), 5.70 (s, 2H), 4.25 (t, J = 6 Hz, 2H), 3.66 (t, J = 6 Hz, 2H), 3.23 (s, 3H); MS (ESI) m/z: 395.2 $[M+H]^+$.

*4.1.13. N-(1-Methyl-1H-pyrazol-4-yl)-1-(4-nitrobenzyl)-1H-pyrazolo[3,4-d]pyrimidin- 6-amine (**11i**)*

Compound **10b** (7.2 g, 25.0 mmol) and **20a** (2.7 g, 27.5 mmol) were reacted using the general procedure to the synthesis of **11i** as a yellow solid, yield 86%, (7.5 g, 21.5 mmol). ^{1}H NMR (300 MHz, DMSO-d_6) δ 9.03 (s, 1H), 8.16 (d, J = 9 Hz, 2H), 8.10 (s, 1H), 8.03 (s, 1H), 7.53 (d, J = 9 Hz, 2H), 7.47 (s, 1H), 5.71 (s, 2H), 3.80 (s, 3H); MS (ESI) m/z: 351.2 $[M+H]^+$.

*4.1.14. N-(1-(3-Nitrobenzyl)-1H-pyrazolo[3,4-d]pyrimidin-6-yl) cyclopropanecarbox- amide (**11j**)*

Compound **10a** (7.2 g, 25.0 mmol) and cyclopropanecarboxamide (2.3 g, 27.5 mmol) were reacted using the general procedure to the synthesis of **11j** as a yellow solid, yield 63%, (5.3 g, 15.7 mmol). ^{1}H NMR (300 MHz, DMSO-d_6) δ 9.00 (s, 1H), 8.24 (m, 1H), 8.16 (m, 1H), 8.06 (s, 1H), 7.63 (d, J = 9 Hz, 1H), 7.56 (t, J = 9 Hz, 1H), 5.69 (s, 2H), 1.70–1.67 (m, 1H) , 0.84–0.73 (m, 4H); MS (ESI) m/z: 339.1 $[M+H]^+$.

General procedure for the synthesis of **12a-12j**

The mixture of **11** (10.0 mmol) and Pd/C (10 wt%, 0.4 g) in EtOH (200 mL) was heated to reflux under argon. Then hydrazine hydrate (85 wt%, 200.0 mmol) was added dropwise to the mixture over 0.5 h maintaining the temperature at 78–80 ℃. After the addition was completed, the reaction mixture was stirred and refluxed for 2 h. The hot solution was then filtered by vacuum through a celite pad. The solvent was concentrated to provide the target compounds without further purification.

*4.1.15. 1-(3-Aminobenzyl)-N-phenyl-1H-pyrazolo[3,4-d]pyrimidin-6-amine (**12a**)*

Compound **11a** (3.5 g, 10.0 mmol) and Pd/C (10 wt%, 0.4 g) were reacted using the general procedure to the synthesis of **12a** as a white solid, yield 97%, (3.1 g, 9.7 mmol). MS (ESI) m/z: 317.2 $[M+H]^+$.

*4.1.16. 1-(3-Aminobenzyl)-N-(4-morpholinophenyl)-1H-pyrazolo[3,4-d] pyrimidin-6- amine (**12b**)*

Compound **11b** (4.3 g, 10.0 mmol) and Pd/C (10 wt%, 0.4 g) were reacted using the general procedure to the synthesis of **12b** as a white solid, yield 96%, (3.9 g, 9.6 mmol). MS (ESI) m/z: 402.2 $[M+H]^+$.

*4.1.17. 1-(3-Aminobenzyl)-N-(4-(4-methylpiperazin-1-yl)phenyl)-1H-pyrazolo[3,4-d] pyrimidin-6-amine (**12c**)*

Compound **11c** (4.4 g, 10.0 mmol) and Pd/C (10 wt%, 0.4 g) were reacted using the general procedure to the synthesis of **12c** as a white solid, yield 95%, (4.2 g, 9.5 mmol). MS (ESI) m/z: 415.3 $[M+H]^+$.

*4.1.18. 1-(4-Aminobenzyl)-N-(4-morpholinophenyl)-1H-pyrazolo[3,4-d] pyrimidin-6- amine (**12d**)*

Compound **11d** (4.3 g, 10.0 mmol) and Pd/C (10 wt%, 0.4 g) were reacted using the general procedure to the synthesis of **12d** as a white solid, yield 92%, (3.7 g, 9.2 mmol). MS (ESI) m/z: 402.2 $[M+H]^+$.

*4.1.19. 1-(4-Aminobenzyl)-N-(4-(4-methylpiperazin-1-yl)phenyl)-1H-pyrazolo[3,4-d] pyrimidin-6-amine (**12e**)*

Compound **11e** (4.4 g, 10.0 mmol) and Pd/C (10 wt%, 0.4 g) were reacted using the general procedure to the synthesis of **12e** as a white solid, yield 95%, (4.2 g, 9.5 mmol). MS (ESI) m/z: 415.3 $[M+H]^+$.

*4.1.20. 1-(3-Aminobenzyl)-N-(1-methyl-1H-pyrazol-4-yl)-1H-pyrazolo [3,4-d]pyramid in-6-amine (**12f**)*

Compound **11f** (3.5 g, 10.0 mmol) and Pd/C (10 wt%, 0.4 g) were reacted using the general procedure to the synthesis of **12f** as a white solid, yield 93%, (3.0 g, 9.3 mmol). MS (ESI) m/z: 321.2 $[M+H]^+$.

*4.1.21. 2-(4-((1-(3-Aminobenzyl)-1H-pyrazolo[3,4-d]pyrimidin-6-yl) amino)-1H-pyraz ol-1-yl)ethanol (**12 g**)*

Compound **11 g** (3.8 g, 10.0 mmol) and Pd/C (10 wt%, 0.4 g) were reacted using the general procedure to the synthesis of **12 g** as a white solid, yield 90%, (3.2 g, 9.0 mmol). MS (ESI) m/z: 351.2 $[M+H]^+$.

*4.1.22. 1-(4-Aminobenzyl)-N-(1-(2-methoxyethyl)-1H-pyrazol-4-yl)-1H-pyrazolo[3,4- d]pyrimidin-6-amine (**12 h**)*

Compound **11 h** (3.9 g, 10.0 mmol) and Pd/C (10 wt%, 0.4 g) were reacted using the general procedure to the synthesis of **12 h** as a white solid, yield 96%, (3.5 g, 9.6 mmol). MS (ESI) m/z: 365.2 $[M+H]^+$.

*4.1.23. 1-(4-Aminobenzyl)-N-(1-methyl-1H-pyrazol-4-yl)-1H-pyrazolo [3,4-d]pyramid in-6-amine (**12i**)*

Compound **11i** (3.5 g, 10.0 mmol) and Pd/C (10 wt%, 0.4 g) were reacted using the general procedure to the synthesis of **12i** as a white solid, yield 96%, (3.1 g, 9.6 mmol). MS (ESI) m/z: 321.2 $[M+H]^+$.

*4.1.24. N-(1-(3-Aminobenzyl)-1H-pyrazolo[3,4-d]pyrimidin-6-yl) cyclopropanecarbox amide (**12j**)*

Compound **11j** (3.4 g, 10.0 mmol) and Pd/C (10 wt%, 0.3 g) were reacted using the general procedure to the synthesis of **12j** as a white solid, yield 90%, (2.8 g, 9.0 mmol). MS (ESI) *m/z*: 309.2 $[M+H]^+$.

General procedure for the synthesis of 13a-13b, 13f-13 h, **13k**, 13n, 13q, 13 t-13w, 14c-14d and 14f

To a solution of **12** (2.0 mmol) in THF (15 mL) were added DIEA (2.2 mmol) and acyl chloride (2.1 mmol) at −5 °C. The resulting mixture was stirred for 30 min. Then it was quenched by MeOH (5 mL), concentrated, and purified by silica gel column chromatography (0–10% MeOH in DCM) to afford the title compounds.

*4.1.25. N-(3-((6-(Phenylamino)-1H-pyrazolo[3,4-d]pyrimidin-1-yl) methyl)phenyl) acrylamide (**13a**)*

Compound **12a** (0.6 g, 2.0 mmol) and acryloyl chloride (0.2 g, 2.1 mmol) were reacted using the general procedure to the synthesis of **13a** as a white solid, yield 80%, (0.6 g, 1.6 mmol); mp: 125–126 °C. ^{1}H NMR (300 MHz, DMSO-d_6) δ 9.12 (s, 1H), 8.22 (s, 1H), 7.83 (s, 1H), 7.80 (s, 1H), 7.66–7.63 (m, 2H), 7.36–7.26 (m, 3H), 7.02–7.01 (m, 2H), 6.54–6.45 (m, 1H), 6.26–6.20 (m, 1H), 5.72–5.68 (m, 1H), 5.49 (s, 2H); ^{13}C NMR (75 MHz, DMSO-d_6) δ 163.30, 155.90, 153.51, 152.30, 139.48, 139.39, 137.30, 135.04, 131.95, 129.00, 128.73, 126.74, 122.79, 122.51, 119.43, 118.75, 118.48, 108.53, 50.03; HRMS (ESI): *m/z* 371.1593 $[M+H]^+$ (Calcd for $C_{21}H_{18}N_6O$, 370.1542).

*4.1.26. N-(3-((6-(phenylamino)-1H-pyrazolo[3,4-d]pyrimidin-1-yl) methyl)phenyl) acrylamide (**13b**)*

Compound **12a** (0.6 g, 2.0 mmol) and 2-butenoyl chloride (0.2 g, 2.1 mmol) were reacted using the general procedure to the synthesis of **13b** as a white solid, yield 87%, (0.7 g, 1.7 mmol); mp: 150–151 °C.^{1}H NMR (300 MHz, DMSO-d_6) δ 9.06 (s, 1H), 8.17 (s, 1H), 7.84 (s, 1H), 7.82 (s, 1H), 7.61–7.54 (m, 2H), 7.34–7.24 (m, 3H), 7.01–6.97 (m, 2H), 6.82–6.70 (m, 1H), 6.15–6.10 (m, 1H), 5.48 (s, 2H), 1.84–1.81 (m, 3H); ^{13}C NMR (75 MHz, DMSO-d_6) δ 163.53, 157.00, 153.52, 153.21, 139.81, 139.76, 139.66, 137.41, 134.33, 128.89, 128.60, 126.01, 122.40, 122.05, 119.18, 118.53, 118.25, 108.54, 49.89, 17.46; MS (ESI) *m/z*: 385.2 $[M+H]^+$.

*4.1.27. N-(3-((6-((4-Morpholinophenyl)amino)-1H-pyrazolo[3,4-d] pyrimidin-1-yl) methyl)phenyl)acrylamide (**13f**)*

Compound **12b** (0.8 g, 2.0 mmol) and acryloyl chloride (0.2 g, 2.1 mmol) were reacted using the general procedure to the synthesis of **13f** as a white solid, yield 84%, (0.8 g, 1.7 mmol); mp: 197–198 °C. ^{1}H NMR (300 MHz, DMSO-d_6) δ 9.07 (s, 1H), 8.18 (s, 1H), 7.98–7.96 (m, 2H), 7.86–7.83 (m, 2H), 7.68–7.66 (m, 2H), 7.30 (t, J = 9 Hz, 1H), 6.99–6.97 (m, 1H), 6.60–6.51 (m, 1H), 6.24–6.19 (m, 1H), 5.72–5.68 (m, 1H), 5.51 (s, 2H), 4.11 (brs, 4H), 3.57 (brs, 4H); ^{13}C NMR (75 MHz, DMSO-d_6) δ 163.35, 157.04, 153.86, 153.30, 139.54, 137.53, 134.27, 132.01, 129.09, 122.68, 121.79, 119.60, 118.35, 109.01, 63.61, 54.21, 50.13; HR-ESIMS: *m/z* 456.2162 $[M+H]^+$ (Calcd for $C_{25}H_{25}N_7O_2$, 455.2070).

*4.1.28. N-(3-((6-((4-Morpholinophenyl)amino)-1H-pyrazolo[3,4-d] pyrimidin-1-yl) methyl)phenyl)propionamide (**13g**)*

Compound **12b** (0.8 g, 2.0 mmol) and propionyl chloride (0.2 g, 2.1 mmol) were reacted using the general procedure to the synthesis of **13g** as a white solid, yield 87%, (0.8 g, 1.7 mmol); mp: 247–248 °C. ^{1}H NMR (300 MHz, DMSO-d_6) δ 9.05 (s, 1H), 8.16 (s, 1H), 7.96 (s, 1H), 7.93 (s, 1H), 7.72–7.70 (m, 2H), 7.56–7.51 (m, 2H), 7.27 (t, J = 9 Hz, 1H), 6.97–6.94 (m, 1H) , 5.49 (s, 2H), 4.05 (brs, 4H), 3.50 (brs, 4H), 2.31–2.24 (m, 2H), 1.05–1.00 (m, 3H); ^{13}C NMR (75 MHz, DMSO-d_6) δ 172.12, 157.37, 154.06, 153.32, 139.76, 137.45, 136.73, 134.06, 128.91, 122.11, 121.32, 120.99, 119.55, 118.27, 117.85, 108.92, 63.75, 53.82, 49.95, 29.46, 9.63; MS (ESI) *m/z*: 458.2 $[M+H]^+$.

*4.1.29. N-(3-((6-((4-Morpholinophenyl)amino)-1H-pyrazolo[3,4-d] pyrimidin-1-yl) methyl)phenyl)but-2-enamide (**13 h**)*

Compound **12b** (0.8 g, 2.0 mmol) and 2-butenoyl chloride (0.2 g, 2.1 mmol) were reacted using the general procedure to the synthesis of **13 h** as a white solid, yield 90%, (0.8 g, 1.8 mmol); mp: 210–211 °C. ^{1}H NMR (300 MHz, DMSO-d_6) δ 9.07 (s, 1H), 8.18 (s, 1H), 7.97–7.94 (m, 2H), 7.80–7.77 (m, 2H), 7.62–7.60 (m, 2H), 7.28 (t, J = 9 Hz, 1H), 6.97–6.95 (m, 1H), 6.82–6.70 (m, 1H), 6.19–6.14 (m, 1H), 5.50 (s, 2H), 4.09 (brs, 4H), 3.54 (brs, 4H), 2.92 (d, J = 9 Hz, 2H); ^{13}C NMR (75 MHz, DMSO-d_6) δ 163.59, 157.27, 154.05, 153.29, 139.91, 139.73, 137.52, 136.54, 134.09, 129.01, 119.55, 118.52, 114.06, 108.97, 63.71, 53.96, 50.08, 17.54; MS (ESI) *m/z*: 470.2 $[M+H]^+$.

*4.1.30. N-(3-((6-((4-(4-Methylpiperazin-1-yl)phenyl)amino)-1H-pyrazolo [3,4-d] pyrimidin-1-yl)methyl)phenyl)acrylamide (**13k**)*

Compound **12c** (0.8 g, 2.0 mmol) and acryloyl chloride (0.2 g, 2.1 mmol) were reacted using the general procedure to the synthesis of **13k** as a white solid, yield 84%, (0.8 g, 1.7 mmol); mp: 186–187 °C. ^{1}H NMR (300 MHz, DMSO-d_6) δ 9.04 (s, 1H), 8.17 (s, 1H), 7.73–7.70 (m, 3H), 7.63–7.60 (m, 1H), 7.43 (s, 1H), 7.31–7.26 (m, 2H), 6.98–6.96 (m, 1H), 6.57–6.49 (m, 1H), 6.25–6.20 (m, 1H), 5.75–5.71 (m, 1H), 5.46 (s, 2H), 3.58 (m, 4H), 3.17 (m, 4H), 2.80 (s, 3H); ^{13}C NMR (75 MHz, DMSO-d_6) δ 163.27, 156.66, 153.58, 152.89, 139.46, 137.48, 134.49, 131.95, 129.02, 128.10, 126.81, 122.59, 120.33, 118.60, 118.36, 116.88, 108.27, 55.08, 51.89, 49.96, 25.13; HRMS (ESI): *m/z* 469.2465 $[M+H]^+$ (Calcd for $C_{26}H_{28}N_8O$, 468.2386).

*4.1.31. N-(3-((6-((1-Methyl-1H-pyrazol-4-yl)amino)-1H-pyrazolo[3,4-d] pyrimidin-1- yl)methyl)phenyl)acrylamide (**13n**)*

Compound **12f** (0.6 g, 2.0 mmol) and acryloyl chloride (0.2 g, 2.1 mmol) were reacted using the general procedure to the synthesis of **13n** as a white solid, yield 82%, (0.6 g, 1.6 mmol); mp: 159–160 °C. ^{1}H NMR (300 MHz, DMSO-d_6) δ 8.92 (s, 1H), 8.07 (s, 1H), 8.04 (s, 1H), 7.62–7.55 (m, 2H), 7.53 (s, 1H), 7.29 (t, J = 6 Hz, 1H), 7.06–7.03 (m, 1H), 6.44–6.35 (m, 1H), 6.25–6.18 (m, 1H), 5.74–5.70 (m, 1H), 5.53 (s, 2H), 3.83 (s, 3H); ^{13}C NMR (75 MHz, DMSO-d_6) δ 163.16, 157.70, 154.14, 153.12, 139.31, 138.06, 133.78, 131.79, 129.64, 129.03, 127.00, 123.00, 122.81, 120.46, 118.49, 118.20, 49.64, 38.74; HRMS (ESI): *m/z* 375.1668 $[M+H]^+$ (Calcd for $C_{19}H_{18}N_8O$, 374.1604).

*4.1.32. N-(3-((6-((1-(2-Hydroxyethyl)-1H-pyrazol-4-yl)amino)-1H-pyrazolo[3,4-d] pyrimidin-1-yl)methyl)phenyl)acrylamide (**13q**)*

Compound **12 g** (0.7 g, 2.0 mmol) and acryloyl chloride (0.2 g, 2.1 mmol) were reacted using the general procedure to the synthesis of **13q** as a white solid, yield 79%, (0.6 g, 1.6 mmol); mp: 182–183 °C. ^{1}H NMR (300 MHz, DMSO-d_6) δ 8.96 (s, 1H), 8.11 (s, 2H), 7.66–7.58 (m, 2H), 7.50–7.41 (m, 1H), 7.33–7.24 (m, 1H), 7.06–7.04 (m, 1H), 6.50–6.41 (m, 1H), 6.24–6.18 (m, 1H), 5.73–5.69 (m, 1H), 5.51 (s, 2H), 4.15 (t, J = 6 Hz, 2H), 3.72 (t, J = 6 Hz, 2H); ^{13}C NMR (75 MHz, DMSO-d_6) δ 163.21, 157.11, 154.04, 153.45, 139.37, 137.76, 134.47, 131.88, 130.04, 129.69, 128.99, 126.81, 122.36, 120.72, 118.59, 118.28, 107.73, 60.29, 54.20, 49.64; HRMS (ESI): *m/z* 405.1793 $[M+H]^+$ (Calcd for $C_{20}H_{20}N_8O_2$, 404.1709).

*4.1.33. N-(3-((6-((1-(2-Hydroxyethyl)-1H-pyrazol-4-yl)amino)-1H-pyrazolo[3,4-d] pyrimidin-1-yl)methyl)phenyl)acrylamide (**13 t**)*

Compound **12 h** (0.7 g, 2.0 mmol) and acryloyl chloride (0.2 g, 2.1 mmol) were reacted using the general procedure to the synthesis of **13t** as a white solid, yield 85%, (0.7 g, 1.7 mmol); mp: 143–144 °C. ^{1}H NMR (300 MHz, DMSO-d_6) δ 8.92 (s, 1H), 8.07 (s, 1H), 8.06 (s, 1H), 7.63–7.53 (m, 3H), 7.28 (t, J = 9 Hz, 1H), 7.05–7.02 (m, 1H), 6.44–6.35 (m, 1H), 6.25–6.19 (m, 1H), 5.73–5.70 (m, 1H), 5.51 (s, 2H), 4.24 (t, J = 6 Hz, 2H), 3.66 (t, J = 6 Hz, 2H), 3.32 (s, 3H); ^{13}C NMR (75 MHz, DMSO-d_6) δ 163.10, 157.71, 154.11, 154.02, 139.26, 137.91,

133.70, 131.75, 129.89, 128.90, 126.77, 122.79, 122.63, 120.22, 118.48, 118.12, 107.68, 70.74, 57.87, 51.19, 49.48; HRMS (ESI): *m/z* 419.1940 $[M+H]^+$ (Calcd for $C_{21}H_{22}N_8O_2$, 418.1866).

*4.1.34. N-(3-((6-((1-(2-Methoxyethyl)-1H-pyrazol-4-yl)amino)-1H-pyrazolo[3,4-d] pyrimidin-1-yl)methyl)phenyl)propionamide (**13u**)*

Compound **12 h** (0.7 g, 2.0 mmol) and propionyl chloride (0.2 g, 2.1 mmol) were reacted using the general procedure to the synthesis of **13u** as a white solid, yield 89%, (0.8 g, 1.8 mmol); mp: 178–179 °C. ^{1}H NMR (300 MHz, DMSO-d_6) δ 9.04 (s, 1H), 8.17 (s, 1H), 8.13 (s, 1H), 7.64 (s, 1H), 7.55–7.52 (m, 2H), 7.23 (t, J = 9 Hz, 1H), 6.99–6.96 (m, 1H), 5.50 (s, 2H), 4.27 (t, J = 6 Hz, 2H), 3.66 (t, J = 6 Hz, 2H), 3.19 (s, 3H), 2.31–2.24 (m, 2H), 1.05–1.00 (m, 3H); ^{13}C NMR (75 MHz, DMSO-d_6) δ 172.14, 158.79, 154.04, 152.39, 139.80, 137.46, 135.03, 129.97, 128.90, 122.17, 121.97, 120.99, 118.30, 117.96, 107.83, 70.73, 57.99, 51.30, 49.80, 29.49, 9.67; MS (ESI) *m/z*: 421.3 $[M+H]^+$.

*4.1.35. N-(3-((6-((1-(2-Methoxyethyl)-1H-pyrazol-4-yl)amino)-1H-pyrazolo[3,4-d] pyrimidin-1-yl)methyl)phenyl)but-2-enamide (**13v**)*

Compound **12 h** (0.7 g, 2.0 mmol) and 2-butenoyl chloride (0.2 g, 2.1 mmol) were reacted using the general procedure to the synthesis of **13v** as a white solid, yield 83%, (0.7 g, 1.7 mmol); mp: 203–204 °C. ^{1}H NMR (300 MHz, DMSO-d_6) δ 8.99 (s, 1H), 8.13 (s, 1H), 7.61–7.51 (m, 3H), 7.25 (t, J = 9 Hz, 1H), 7.01–6.99 (m, 1H), 6.78–6.71 (m, 1H), 6.14–6.09 (m, 1H), 5.51 (s, 2H), 4.26 (t, J = 6 Hz, 2H), 3.65 (t, J = 6 Hz, 2H), 3.19 (s, 3H), 1.83 (t, J = 9 Hz, 2H); ^{13}C NMR (75 MHz, DMSO-d_6) δ 163.54, 157.86, 154.08, 153.17, 139.84, 139.69, 137.69, 134.47, 129.81, 128.93, 126.01, 122.37, 120.73, 119.54, 118.46, 118.15, 106.80, 70.76, 57.96, 51.26, 49.61, 17.54; MS (ESI) *m/z*: 433.2 $[M+H]^+$.

*4.1.36. N-(1-(3-Acrylamidobenzyl)-1H-pyrazolo[3,4-d]pyrimidin-6-yl) cyclopropane- carboxamide (**13w**)*

Compound **12j** (0.6 g, 2.0 mmol) and acryloyl chloride (0.2 g, 2.1 mmol) were reacted using the general procedure to the synthesis of **13w** as a white solid, yield 75%, (0.5 g, 1.5 mmol); mp: 121–122 °C. ^{1}H NMR (300 MHz, DMSO-d_6) δ 8.94 (s, 1H), 8.06 (s, 1H), 7.63–7.60 (m, 1H), 7.56 (s, 1H), 7.31–7.26 (m, 1H), 7.04–7.01 (m, 1H), 6.48–6.39 (m, 1H), 6.22–6.16 (m, 1H), 5.70–5.66 (m, 1H), 5.49 (s, 2H), 1.75–1.69 (m, 1H) , 0.79–0.76 (m, 4H); ^{13}C NMR (75 MHz, DMSO-d_6) δ 172.15, 163.15, 154.92, 154.24, 150.52, 139.24, 135.09, 134.05, 131.79, 128.95, 126.93, 122.36, 120.15, 117.83, 105.54, 60.04, 14.92, 8.10; MS (ESI) *m/z*: 363.2 $[M+H]^+$

*4.1.37. N-(4-((6-((4-Morpholinophenyl)amino)-1H-pyrazolo[3,4-d] pyrimidin-1-yl) methyl)phenyl)acrylamide (**14c**)*

Compound **12d** (0.8 g, 2.0 mmol) and acryloyl chloride (0.2 g, 2.1 mmol) were reacted using the general procedure to the synthesis of **14c** as a white solid, yield 89%, (0.8 g, 1.8 mmol); mp: 138–139 °C. ^{1}H NMR (300 MHz, DMSO-d_6) δ 9.05 (s, 1H), 8.16 (s, 1H), 7.97–7.94 (m, 2H), 7.78–7.75 (m, 2H), 7.69–7.66 (m, 2H), 7.40 (s, 1H), 7.28–7.25 (m, 2H), 6.54–6.45 (m, 1H), 6.25–6.19 (m, 1H), 5.73–5.70 (m, 1H), 5.50 (s, 2H), 4.08 (brs, 4H), 3.55 (brs, 4H); ^{13}C NMR (75 MHz, DMSO-d_6) δ 163.20, 157.29, 154.03, 153.21, 139.09, 138.57, 136.04, 133.99, 131.90, 128.22, 126.83, 123.70, 121.31, 119.56, 114.09, 108.99, 63.81, 53.83, 49.76; HRMS (ESI): *m/z* 456.2146 $[M+H]^+$ (Calcd for $C_{25}H_{25}N_7O_2$, 455.2070).

*4.1.38. N-(4-((6-((4-(4-Methylpiperazin-1-yl)phenyl)amino)-1H-pyrazolo [3,4-d] pyrimidin-1-yl)methyl)phenyl)acrylamide (**14d**)*

Compound **12e** (0.8 g, 2.0 mmol) and acryloyl chloride (0.2 g, 2.1 mmol) were reacted using the general procedure to the synthesis of **14d** as a white solid, yield 81%, (0.8 g, 1.6 mmol); mp: 147–148 °C. ^{1}H NMR (300 MHz, DMSO-d_6) δ 9.06 (s, 1H), 8.16 (s, 1H), 7.85–7.82 (m, 2H), 7.69–7.64 (m, 1H), 7.40 (s, 1H), 7.27–7.25 (m, 2H), 6.54–6.45 (m, 1H), 6.24–6.19 (m, 1H), 5.72–5.69 (m, 1H), 5.42 (s, 2H), 3.59 (s, 4H), 3.16 (s, 4H), 2.80 (s, 2H); ^{13}C NMR (75 MHz, DMSO-d_6) δ 163.18, 157.21, 154.08, 153.25, 140.49, 138.57, 137.13, 131.93, 128.42, 128.19, 126.75, 121.68, 119.45, 116.84, 108.12, 54.01, 50.80, 49.76, 29.44; HRMS (ESI): *m/z* 469.2446 $[M+H]^+$ (Calcd for $C_{26}H_{28}N_8O$, 468.2386).

*4.1.39. N-(4-((6-((4-(4-Methylpiperazin-1-yl)phenyl)amino)-1H-pyrazolo [3,4-d] pyrimidin-1-yl)methyl)phenyl)acrylamide (**14f**)*

Compound **12i** (0.6 g, 2.0 mmol) and acryloyl chloride (0.2 g, 2.1 mmol) were reacted using the general procedure to the synthesis of **14f** as a white solid, yield 87%, (0.6 g, 1.7 mmol); mp: 112–114 °C. ^{1}H NMR (300 MHz, DMSO-d_6) δ 9.01 (s, 1H), 8.14 (s, 1H), 8.06 (s, 1H), 7.68–7.63 (m, 2H), 7.39 (s, 2H), 7.27–7.25 (m, 1H), 6.56–6.47 (m, 1H), 6.24–6.19 (m, 1H), 5.71–5.68 (m, 1H), 5.59 (s, 1H), 5.50 (s, 1H), 3.85 (s, 3H); ^{13}C NMR (75 MHz, DMSO-d_6) δ 163.20, 157.24, 154.11, 152.61, 138.64, 137.08, 134.86, 131.97, 131.23, 129.72, 128.91, 128.22, 126.68, 123.70, 122.28, 119.46, 107.79, 49.52, 38.78; HRMS (ESI): *m/z* 375.1686 $[M+H]^+$ (Calcd for $C_{19}H_{18}N_8O$, 374.1604).

General procedure for the synthesis of 13c, 13i, 13 l, 13o, 13r, 14a and 14e

To a stirred solution of **12** (2.0 mmol) in MeOH (20 mL) was added KOAc (3.0 mmol) and BrCN (2.2 mmol) at 0 °C. The reaction mixture was stirred at room temperature for 16 h. It was quenched with water, and was evaporated to dryness. The crude mass was purified by silica gel column chromatography (0–10% MeOH in DCM) to afford the title compounds.

*4.1.40. N-(3-((6-((4-Morpholinophenyl)amino)-1H-pyrazolo[3,4-d] pyrimidin-1-yl) methyl)phenyl)cyanamide (**13c**)*

Compound **12b** (0.8 g, 2.0 mmol) was reacted using the general procedure to the synthesis of **13c** as a white solid, yield 75%, (0.6 g, 1.5 mmol); mp: 196–198 °C. ^{1}H NMR (300 MHz, DMSO-d_6) δ 8.94 (s, 1H), 8.08 (s, 1H), 7.70–7.67 (m, 3H), 7.54–7.51 (m, 1H), 7.43–7.41 (m, 1H), 7.31 (t, J = 9 Hz, 1H), 6.88–6.85 (m, 1H), 5.47 (s, 2H), 4.13 (t, J = 6 Hz, 1H), 3.73 (brs, 4H), 3.04 (brs, 4H); ^{13}C NMR (75 MHz, DMSO-d_6) δ 158.22, 154.09, 153.79, 139.10, 138.92, 136.19, 133.79, 130.12, 128.67, 124.65, 121.71, 120.12, 115.57, 114.54, 108.10, 66.17, 54.63, 49.19; MS (ESI) *m/z*: 427.2 $[M+H]^+$

*4.1.41. N-(3-((6-((4-(4-Methylpiperazin-1-yl)phenyl)amino)-1H-pyrazolo [3,4-d] pyrimidin-1-yl)methyl)phenyl)cyanamide (**13i**)*

Compound **12c** (0.8 g, 2.0 mmol) was reacted using the general procedure to the synthesis of **13i** as a white solid, yield 79%, (0.7 g, 1.6 mmol); mp: 240–241 °C. ^{1}H NMR (300 MHz, DMSO-d_6) δ 8.96 (s, 1H), 8.09 (s, 1H), 7.74 (s, 1H), 7.71 (s, 1H), 7.31 (t, J = 9 Hz, 1H), 6.99–6.96 (m, 2H), 6.94–6.86 (m, 2H), 5.47 (s, 2H), 3.44 (s, 4H), 3.32 (s, 4H), 2.84 (s, 3H); ^{13}C NMR (75 MHz, DMSO-d_6) δ 161.18, 158.20, 154.20, 153.77, 144.61, 139.12, 138.99, 133.89, 133.46, 130.18, 121.72, 120.13, 116.62, 114.21, 113.82, 108.26, 52.48, 52.04, 49.41, 46.45, 42.24, 29.06; MS (ESI) *m/z*: 440.3 $[M+H]^+$.

*4.1.42. N-(3-((6-((1-Methyl-1H-pyrazol-4-yl)amino)-1H-pyrazolo[3,4-d] pyrimidin- 1-yl)methyl)phenyl)cyanamide (**13 l**)*

Compound **12f** (0.6 g, 2.0 mmol) was reacted using the general procedure to the synthesis of **13 l** as a white solid, yield 73%, (0.5 g, 1.5 mmol); mp: 191–193 °C. ^{1}H NMR (300 MHz, DMSO-d_6) δ 8.92 (s, 1H), 8.06 (s, 1H), 8.03 (s, 1H), 7.55 (s, 1H), 7.31 (t, J = 9 Hz, 1H), 6.98–6.96 (m, 1H), 6.88–6.80 (m, 2H), 5.54 (s, 2H), 3.83 (s, 3H); ^{13}C NMR (75 MHz, DMSO-d_6) δ 157.71, 154.18, 154.06, 139.22, 138.90, 133.79, 130.00, 129.73, 122.96, 121.73, 120.51, 114.09, 113.79, 111.75, 49.25, 38.69; MS (ESI) *m/z*: 346.1 $[M+H]^+$.

*4.1.43. N-(3-((6-((1-(2-Hydroxyethyl)-1H-pyrazol-4-yl)amino)-1H-pyrazolo[3,4-d] pyrimidin-1-yl)methyl)phenyl)cyanamide (**13o**)*

Compound **12 g** (0.7 g, 2.0 mmol) was reacted using the general procedure to the synthesis of **13o** as a white solid, yield 52%, (0.4 g, 1.0 mmol); mp: 240–242 °C. ^{1}H NMR (300 MHz, DMSO-d_6) δ 8.88 (s, 1H), 8.06 (s, 1H), 8.02 (s, 1H), 7.61 (s, 1H), 7.53 (s, 1H), 7.36 (t, J = 9 Hz, 1H), 7.13 (s, 1H), 7.04–7.02 (m, 1H), 5.54 (s, 2H), 4.15 (t, J = 6 Hz, 2H), 3.74 (t, J = 6 Hz, 2H); ^{13}C NMR (75 MHz, DMSO-d_6) δ 157.50, 154.20, 153.92, 139.18, 137.44, 133.16, 130.05, 129.55, 128.71, 125.04, 122.67, 120.33, 117.08, 113.96, 107.67, 60.38, 54.32, 49.39; MS (ESI) *m/z*: 376.2 $[M+H]^+$.

*4.1.44. N-(3-((6-((1-(2-Methoxyethyl)-1H-pyrazol-4-yl)amino)-1H-pyrazolo[3,4-d] pyrimidin-1-yl)methyl)phenyl)cyanamide (**13r**)*

Compound **12 h** (0.7 g, 2.0 mmol) was reacted using the general procedure to the synthesis of **13r** as a white solid, yield 79%, (0.6 g, 1.6 mmol); mp: 275–276 °C. ^{1}H NMR (300 MHz, DMSO-d_6) δ 8.92 (s, 1H), 8.09 (s, 1H), 8.07 (s, 1H), 7.57 (s, 1H), 7.49 (t, J = 9 Hz, 1H), 7.36 (s, 1H), 7.30 (t, J = 9 Hz, 1H), 7.08–7.06 (m, 1H), 5.52 (s, 2H), 4.24 (t, J = 6 Hz, 3H), 3.84 (s, 3H), 3.66 (t, J = 6 Hz, 3H), 3.20 (s, 3H); ^{13}C NMR (75 MHz, DMSO-d_6) δ 161.05, 157.73, 154.14, 153.12, 138.67, 138.18, 133.83, 131.60, 129.50, 129.14, 123.02, 122.82, 120.24, 118.35, 115.87, 107.60, 70.80, 57.95, 51.25, 49.43, 26.71; MS (ESI) *m/z*: 390.2 $[M+H]^+$.

*4.1.45. N-(4-((6-((4-morpholinophenyl)amino)-1H-pyrazolo[3,4-d] pyrimidin-1-yl) methyl)phenyl)cyanamide (**14a**)*

Compound **12d** (0.8 g, 2.0 mmol) was reacted using the general procedure to the synthesis of **14a** as a white solid, yield 70%, (0.6 g, 1.4 mmol); mp: 208–210 °C. ^{1}H NMR (300 MHz, DMSO-d_6) δ 8.93 (s, 1H), 8.04 (s, 1H), 7.71–7.69 (m, 2H), 7.30–7.27 (m, 2H), 6.94–6.92 (m, 3H), 5.42 (s, 2H), 3.74 (brs, 4H), 3.05 (brs, 4H); ^{13}C NMR (75 MHz, DMSO-d_6) δ 158.19, 153.99, 153.62, 141.94, 138.10, 133.60, 132.67, 131.31, 129.30, 120.13, 115.57, 115.09, 111.96, 108.20, 66.17, 54.44, 49.20; MS (ESI) *m/z*: 427.2 $[M+H]^+$.

*4.1.46. N-(4-((6-((1-Methyl-1H-pyrazol-4-yl)amino)-1H-pyrazolo[3,4-d] pyrimidin-1- yl)methyl)phenyl)cyanamide (**14e**)*

Compound **12i** (0.6 g, 2.0 mmol) was reacted using the general procedure to the synthesis of **14e** as a white solid, yield 77%, (0.5 g, 1.5 mmol); mp: 169–171 °C. ^{1}H NMR (300 MHz, DMSO-d_6) δ 9.01 (s, 1H), 8.14 (s, 1H), 8.06 (s, 1H), 7.68–7.63 (m, 2H), 7.39 (s, 2H), 7.27–7.25 (m, 1H), 6.56–6.47 (m, 1H), 6.24–6.19 (m, 1H), 5.71–5.68 (m, 1H), 5.59 (s, 2H), 3.85 (s, 3H); ^{13}C NMR (75 MHz, DMSO-d_6) δ 163.20, 157.24, 154.11, 152.61, 138.64, 137.08, 134.86, 131.97, 131.23, 129.72, 128.91, 128.22, 126.68, 123.70, 122.28, 119.46, 107.79, 49.52, 38.78; MS (ESI) *m/z*: 346.2 $[M+H]^+$.

General procedure for the synthesis of 13d, 13j, 13 m, 13p, **13s** and 14b

To a stirred solution of **12** (2.0 mmol) in DMF (10 mL) was added DIPEA (10.4 mg, 2.0 mmol), HATU (5.0 mmol), and 2-cyanoacetic acid (2.5 mmol) at 0 °C. The reaction mixture was stirred at room temperature for 16 h. It was quenched with water and extracted with ethyl acetate (3 × 50 mL). The organic layer was washed with water (2 × 30 mL) followed by brine (1 × 30 mL), dried over anhydrous sodium sulfate, and was evaporated to dryness. The crude mass was purified by silica gel column chromatography (0–10% MeOH in DCM) to afford the title compounds.

*4.1.47. 2-Cyano-N-(3-((6-((4-morpholinophenyl)amino)-1H-pyrazolo [3,4-d]pyrimidin −1-yl)methyl)phenyl)acetamide (**13d**)*

Compound **12b** (0.8 g, 2.0 mmol) was reacted using the general procedure to the synthesis of **13d** as a pale yellow solid, yield 67%, (0.6 g, 1.3 mmol); mp: 175–177 °C. ^{1}H NMR (300 MHz, DMSO-d_6) δ 8.93 (s, 1H), 8.06 (s, 1H), 7.72 (s, 1H), 7.69 (s, 1H), 7.49–7.47 (m, 1H), 7.42 (s, 1H), 7.30 (t, J = 9 Hz, 1H), 7.05–7.02 (m, 1H), 6.93 (s, 1H), 6.90 (s, 1H), 5.46 (s, 2H), 3.85 (s, 2H), 3.74 (brs, 4H), 3.05 (brs, 4H); ^{13}C NMR (75 MHz, DMSO-d_6) δ 161.00, 158.21, 153.94, 153.77, 138.65, 137.98, 133.69, 132.69, 129.11, 123.05, 120.10, 118.34, 118.01, 115.78, 115.59, 108.13, 66.18, 59.74, 54.85, 49.23; MS (ESI) *m/z*:469.2 $[M+H]^+$.

*4.1.48. 2-Cyano-N-(3-((6-((4-(4-methylpiperazin-1-yl)phenyl)amino)-1H-pyrazolo [3,4-d]pyrimidin-1-yl)methyl)phenyl)acetamide (**13j**)*

Compound **12c** (0.8 g, 2.0 mmol) was reacted using the general procedure to the synthesis of **13j** as a pale yellow solid, yield 64%, (0.6 g, 1.3 mmol); mp: 208–210 °C. ^{1}H NMR (300 MHz, $CDCl_3$) δ 8.74 (s, 1H), 8.16 (s, 1H), 7.87 (s, 1H), 7.58 (s, 1H), 7.55 (s, 1H), 7.44 (m, 2H), 7.27 (s, 1H), 7.14–7.11 (m, 1H), 6.96–6.93 (m, 1H), 5.45 (s, 2H), 3.46 (s, 2H), 3.19 (s, 4H), 2.62 (s, 4H), 2.38 (s, 3H); ^{13}C NMR (75 MHz, $CDCl_3$) δ 161.75, 157.14, 154.47, 153.72, 139.13, 137.29, 136.03, 133.81, 129.73, 125.09, 121.13, 120.68, 119.98, 117.04, 113.28, 108.97, 55.21, 50.97, 49.74, 29.83, 26.93; MS (ESI) *m/z*: 482.2 $[M+H]^+$.

*4.1.49. 2-Cyano-N-(3-((6-((1-methyl-1H-pyrazol-4-yl)amino)-1H-pyrazolo[3,4-d] pyrimidin-1-yl)methyl)phenyl)acetamide (**13 m**)*

Compound **12f** (0.6 g, 2.0 mmol) was reacted using the general procedure to the synthesis of **13 m** as a pale yellow solid, yield 56%, (0.4 g, 1.1 mmol); mp: 162–164 °C. ^{1}H NMR (300 MHz, DMSO-d_6) δ 8.92 (s, 1H), 8.06 (s, 1H), 8.04 (s, 1H), 7.54 (s, 1H), 7.50–7.48 (m, 1H), 7.39 (s, 1H), 7.31 (t, J = 9 Hz, 1H), 7.10–7.08 (m, 1H), 5.54 (s, 2H), 3.83 (s, 3H) , 3.39 (s, 2H); ^{13}C NMR (75 MHz, DMSO-d_6) δ 161.14, 157.72, 154.18, 152.41, 138.71, 138.27, 133.86, 129.21, 123.21, 123.03, 120.55, 118.39, 118.06, 115.95,107.62, 49.58, 38.80, 26.77; HRMS (ESI): *m/z* 388.1633 $[M+H]^+$ (Calcd for $C_{19}H_{17}N_9O$, 387.1556).

*4.1.50. 2-Cyano-N-(3-((6-(((1-(2-hydroxyethyl)-1H-pyrazol-4-yl)amino)-1H-pyrazolo [3,4-d]pyrimidin-1-yl)methyl)phenyl)acetamide (**13p**)*

Compound **12 g** (0.7 g, 2.0 mmol) was reacted using the general procedure to the synthesis of **13p** as a pale yellow solid, yield 43%, (0.4 g, 0.9 mmol); mp: 220–221 °C. ^{1}H NMR (300 MHz, DMSO-d_6) δ 8.91 (s, 1H), 8.08 (s, 1H), 8.06 (s, 1H), 7.57 (s, 1H), 7.55–7.52 (m, 1H), 7.49 (s, 1H), 7.28 (t, J = 9 Hz, 1H), 7.06 (m, 1H), 5.50 (s, 2H), 4.12 (t, J = 6 Hz, 2H), 3.96 (s, 3H), 3.72 (t, J = 6 Hz, 2H); ^{13}C NMR (75 MHz, DMSO-d_6) δ 161.13, 157.70, 154.15, 152.26, 138.81, 138.08, 133.80, 129.77, 129.10, 128.49, 123.10, 122.70, 120.37, 118.14, 116.03, 107.54, 60.37, 54.20, 49.52, 26.56; MS (ESI) *m/z*: 418.2 $[M+H]^+$.

*4.1.51. 2-Cyano-N-(3-((6-(((1-(2-methoxyethyl)-1H-pyrazol-4-yl)amino)-1H-pyrazolo [3,4-d]pyrimidin-1-yl)methyl)phenyl)acetamide (**13s**)*

Compound **12 h** (0.7 g, 2.0 mmol) was reacted using the general procedure to the synthesis of **13s** as a pale yellow solid, yield 66%, (0.6 g, 1.3 mmol); mp: 243–245 °C. ^{1}H NMR (300 MHz, DMSO-d_6) δ 8.92 (s, 1H), 8.09 (s, 1H), 8.07 (s, 1H), 7.57 (s, 1H), 7.51–7.45 (m, 1H), 7.36 (s, 1H), 7.30 (t, J = 9 Hz, 1H), 7.08–7.06 (m, 1H), 5.52 (s, 2H), 4.24 (t, J = 6 Hz, 2H), 3.84 (s, 2H), 3.66 (t, J = 6 Hz, 2H), 3.20 (s, 3H); ^{13}C NMR (75 MHz, DMSO-d_6) δ 161.05, 157.73, 154.14, 153.12, 138.67, 138.18, 133.83, 131.60, 129.50, 129.14, 123.02, 122.82, 120.24, 118.35, 115.87, 107.60, 70.80, 57.95, 51.25, 49.43, 26.71; MS (ESI) *m/z*: 432.2 $[M+H]^+$.

*4.1.52. 2-Cyano-N-(4-((6-((4-morpholinophenyl)amino)-1H-pyrazolo [3,4-d]pyrimidin −1-yl)methyl)phenyl)acetamide (**14b**)*

Compound **12d** (0.8 g, 2.0 mmol) was reacted using the general procedure to the synthesis of **14b** as a pale yellow solid, yield 70%, (0.7 g, 1.4 mmol); mp: 197–199 °C. ^{1}H NMR (300 MHz, DMSO-d_6) δ 8.93 (s, 1H), 8.05 (s, 1H), 7.71–7.68 (m, 2H), 7.52–7.49 (m, 2H), 7.27–7.24 (m, 2H), 6.93–6.90 (m, 2H), 5.43 (s, 2H), 3.87 (brs, 2H), 3.74 (brs, 4H), 3.05 (s, 4H); ^{13}C NMR (75 MHz, DMSO-d_6) δ 161.00, 158.17,

154.00, 153.67, 138.83, 137.74, 136.02, 133.60, 132.65, 132.57, 130.26, 128.30, 124.44, 120.10, 119.36, 115.87, 115.56, 108.18, 66.17, 52.58, 49.19, 26.67; MS (ESI) *m/z*: 469.2 $[M+H]^+$.

*4.1.53. 2,2,2-Trifluoro-N-(3-((6-((4-morpholinophenyl)amino)-1H-pyrazolo[3,4-d] pyrimidin-1-yl)methyl)phenyl)acetamide (**13e**)*

To a solution of **12b** (0.8 g, 2.0 mmol) and Et_3N (0.3 g, 3.0 mmol) in THF (80 mL) was added trifluoroacetic anhydride (0.5 g, 2.2 mmol) at 0 ℃. The mixture was stirred at room temperature for 12 h. To the mixture was added DCM (100 mL). The mixture was washed with saturated $NaHCO_3$ solution (50 mL), dried over anhydrous sodium sulfate, and the solvent was evaporated under reduced pressure. The residue was purified by silica gel column chromatography (0–20% MeOH in DCM) to give **13e** as a yellow solid, yield 72%, (0.7 g, 1.4 mmol); mp: 112–114 ˚C. ^{1}H NMR (300 MHz, $CDCl_3$) δ 8.74 (s, 1H), 8.00 (s, 1H), 7.78 (s, 1H), 7.59 (s, 2H), 7.56 (s, 1H), 7.32–7.28 (m, 2H), 7.23–7.22 (m, 1H), 7.08–7.05 (m, 1H), 5.43 (s, 2H), 4.03 (brs, 4H), 3.29 (brs, 4H); ^{13}C NMR (75 MHz, $CDCl_3$) δ 158.03, 155.11, 154.07 (q, J = 38.3), 153.27, 141.28, 139.65, 136.72, 135.27, 130.48, 129.72, 121.04, 120.60, 119.40, 115.07, 115.89(q, J = 287.3), 114.42, 108.96, 65.19, 52.86, 50.60; MS (ESI) *m/z*: 498.2 $[M+H]^+$.

*4.1.54. 4-(4-Nitrophenyl)morpholine (**16a**)*

To a solution of **15** (1.4 g, 10.0 mmol) and K_2CO_3 (1.5 g, 11.0 mmol) in DMSO (10 mL) was added morpholine (0.9 g, 10.0 mmol). The mixture was stirred at 120 ℃ for 6 h. To the mixture was added EtOH/H_2O (26 mL, v/v, 1/1), the solids were collected by filtration, and rinsed with 10 mL of cold EtOH/H_2O (v/v, 1/1) to provide **16a** as a yellow solid, yield 93%, (1.9 g, 9.3 mmol). MS (ESI) *m/z*: 209.1 $[M+H]^+$.

*4.1.55. 1-Methyl-4-(4-nitrophenyl)piperazine (**16b**)*

Compound **15** (1.4 g, 10.0 mmol) and 1-methylpiperazine (1.0 g, 10.0 mmol) were reacted using a procedure similar to the synthesis of **16a**, affording compound **16b** , yield 87%, (1.9 g, 8.7 mmol). MS (ESI) *m/z*: 222.1 $[M+H]^+$.

General procedure for the synthesis of 17b-17c

The mixture of **16** (10.0 mmol) and Pd/C (10 wt%, 0.2 g) in EtOH (200 mL) was heated to reflux under argon. Then hydrazine hydrate (85 wt%, 200.0 mmol) was added dropwise to the mixture over 0.5 h maintaining the temperature at 78–80 ˚C. After the addition was completed, the reaction mixture was stirred and refluxed for 2 h. The hot solution was then filtered by vacuum through celite pad. The solvent was concentrated to provide the target compounds without further purificationas.

*4.1.56. 4-Morpholinoaniline (**17b**)*

Compound **16a** (2.1 g, 10.0 mmol) and Pd/C (10 wt%, 0.2 g) were reacted using the general procedure to the synthesis of **17b** as a yellow solid, yield 98%, (1.8 g, 9.8 mmol). MS (ESI) *m/z*: 179.1 $[M+H]^+$.

*4.1.57. 4-Morpholinoaniline (**17c**)*

Compound **16b** (2.2 g, 10.0 mmol) and Pd/C (10 wt%, 0.2 g) were reacted using the general procedure to the synthesis of **17c** as a yellow solid , yield 99%, (1.9 g, 9.9 mmol). MS (ESI) *m/z*: 192.1 $[M+H]^+$.

*4.1.58. 1-Methyl-4-nitro-1H-pyrazole (**19a**)*

To a solution of compound **18** (1.1 g, 10.0 mmol) and K_2CO_3 (2.1 g, 15.0 mmol) in MeCN (20 mL) was added iodomethane (1.6 g, 11.0 mmol) at room temperature. The reaction mixture was stirred overnight at 82 ˚C. TLC showed the completion of the reactin. The resulting mixture was removed under vacuum. Water (20 mL) was added to the residue, and the resultant mixture was extracted with EtOAc (2 × 50 mL). The organic layers were then washed with water followed by brine. The organic layers were dried over anhydrous sodium sulfate, filtered, and concentrated to provide **19a** as a yellow solid(1.2 g, 9.8 mmol, 98%) without further purification. MS (ESI) *m/z*: 128.1 $[M+H]^+$.

*4.1.59. 2-(4-Nitro-1H-pyrazol-1-yl)ethanol (**19b**)*

Compound **18** (2.2 g, 10.0 mmol) and 2-bromoethanol (1.4 g, 11.0 mmol) were reacted using the general procedure to the synthesis of **19b** as a yellow solid, yield 93%, (1.5 g, 9.3 mmol). MS (ESI) *m/z*: 158.1 $[M+H]^+$.

*4.1.60. 1-(2-Methoxyethyl)-4-nitro-1H-pyrazole (**19c**)*

Compound **18** (2.2 g, 10.0 mmol), KI (0.04 g, 0.3 mmol) and 1-bromo-2-methoxyethane (1.5 g, 11.0 mmol) were reacted using the general procedure to the synthesis of **19c** as a yellow solid, yield 98%, (1.7 g, 9.8 mmol). MS (ESI) *m/z*: 172.1 $[M+H]^+$.

*4.1.61. 1-Methyl-1H-pyrazol-4-amine (**20a**)*

To a solution of compound **19a** (6.4 g, 50.0 mmol) and Pd/C (10 wt %, 0.6 g) in ethanol (50 mL) was stirred at room temperature under a hydrogen atmosphere for 2 days. The reaction mixture was then filtered through Celite and concentrated to provide **20a** as a yellow solid (5.2 g, 46.5 mmol, 93%) without further purification. MS (ESI) *m/z*: 98.1 $[M+H]^+$.

*4.1.62. 2-(4-Amino-1H-pyrazol-1-yl)ethanol (**20b**)*

Compound **19b** (7.9 g, 50.0 mmol) was reacted using the general procedure to the synthesis of **20b** as a yellow solid, yield 96%, (6.1 g, 48.0 mmol). MS (ESI) *m/z*: 128.1 $[M+H]^+$.

*4.1.63. 1-(2-Methoxyethyl)-1H-pyrazol-4-amine (**20c**)*

Compound **19c** (8.6 g, 50.0 mmol) was reacted using the general procedure to the synthesis of **20c** as a yellow solid, yield 96%, (6.8 g, 48.0 mmol). MS (ESI) *m/z*: 142.1 $[M+H]^+$.

4.2. Bioactivity

4.2.1. Kinase enzymatic assays

Human JAK1-3 kinases were obtained from Invitrogen and assays were performed using the HTRF detection technology. Briefly, the enzyme reaction was run in reaction buffer, which consisted of 50 mM HEPES (pH 7.5), 5 mM magnesium chloride ($MgCl_2$) and 1 mM dithiothreitol (DTT). The assay was done by a 384-well plate (10 μL) assay format. The end concentration of enzyme, TK-substrate-biotin, ATP was 1 ng/μl, 1 μM, 3.92 μM for JAK1, 0.004 *n*g/μl, 1 μM, 3.96 μM for JAK2, 0.012 *n*g/μl, 1 μM, 1.43 μM for JAK3, respectively. Compounds were screened at serial diluted concentration in the presence of 2% DMSO with a 5 min pre-incubation of kinase and compounds. All reactions were started by the addition of ATP and TK-substrate-biotin, incubated at 30 ˚C for 60 min and quenched with the stop buffer containing 25 nM Strep-XL665 and TK Ab-Cryptate. The plates were incubated for 60 min. Time-resolved fluorescence was monitored with a Synergy H1 (Biotek) by excitation at 330 nm and emission donor at 620 nm or emission acceptor at 665 nm, respectively. The files recorded by the Synergy H1 were read with Excel and contained the acceptor and donor counts for each sample. And IC_{50} values were determined using the Graphpad Prism 5.0 Software.

4.2.2. Cellular activity assay

Human IL-4 dependent THP-1 cell line (ATCC TIB-202), GM-CSF dependent TF-1 cell line (ATCC CRL-2003) and HEL cell line (ATCC CCL-2) were cultured in RPMI 1640 medium Glutamax (Gibco BRL, Gaithesburg, MD, USA), supplemented with 10% fetal bovine serum (FBS) at 37 ˚C and 5% CO_2. THP-1 cells (ATCC TIB-202) and TF-1 cells (ATCC CRL-2003) were preincubated with the compound at 37 ˚C for 1 h, incubated with IL-4 and GM-CSF at 37 ˚C for 1 h. HEL cell line were

seeded at 2000–5000 cells/well in 96-well plates and maintained for 24 h. The cells were then treated with various concentrations of test compounds for 48 h. The plates were processed using Cell Titer-Glo assay (Promega, Madison, WI, USA), following the manufacturer's instruction. The data were calculated using GraphPad Prim version 5.0. Dose-response curves were fitted using a nonlinear regression model with a sigmoidal dose–response.

4.2.3. Western blotting assay

STAT6 phosphorylation induced by IL-4.

THP-1 cells (ATCC TIB-202) were preincubated with the compound at 37 °C for 1 h, incubated with IL-4 (10 ng/mL) at 37 °C for 60 min, and processed for Western blotting analysis.

STAT5 phosphorylation induced by IL-2.

NK-92 cells (ATCC CRL-2407) were IL-2 starved overnight, preincubated with compound at 37 °C for 1 h, stimulated with IL-2 (1 ng/mL) at 37 °C for 20 min, and processed for Western blotting analysis.

STAT3 phosphorylation induced by IL-6.

TF-1 cells (ATCC CRL-2003) were cultured in media for 18 h without GM-CSF prior to being plated in 24-well plates. The compound was added to the cells, and incubated for 30 min. Cells were then stimulated by IL-6 (400 ng/mL) incubation for 30 min and processed for Western blotting analysis.

STAT5 phosphorylation induced by Prolactin.

22Rv1 cells (ATCC CW22Rv) were starved overnight, preincubated with the compound at 37 °C for 1 h, stimulated with prolactin (500 ng/mL) at 37 °C for 20 min, and processed for Western blotting analysis.

STAT5 phosphorylation induced by GM-CSF.

TF-1 cells (ATCC CRL-2003) were starved overnight in RPMI 1640 medium with 0.1% FBS, preincubated with the compound at 37 °C for 1 h, stimulated with GM-CSF (100 ng/mL) at 37 °C for 20 min, and processed for Western blotting analysis.

Western Blot.

The lysates from THP-1, NK-92, TF-1 and 22Rv1 cells in different groups were extracted and centrifuged at 12,000 g for 15 min at 4 °C, then the total proteins were obtained. An aliquot (50 μg protein) was loaded onto a 8%-12% SDS-PAGE gels and separated electrophoretically. Then the target proteins were transferred to a PVDF membrane (Millipore, USA). After blocking the PVDF membrane in 5% dried skim milk (Boster Biological Technology, China) for 3 h at room temperature, the membrane was incubated overnight at 4 °C with primary antibodies for 3 h at room temperature. Protein detection was performed based on an enhanced chemiluminescence (ECL) method and photographed by using a BioSpectrum Gel Imaging System (HR410, UVP, USA).

4.2.4. Lymphocytes proliferation assays

Spleen cells from male Lewis rats were suspended in RPMI1640 medium, supplemented with 10% fetal calf serum. 100 U/mL penicillin, 100 μg/mL streptomycin, and 50 μM 2-mercaptoethanol at a density of 1.5×10^6 cells/mL. Concanavalin A (Sigma) was used to evaluate *T*-cell proliferation. Rat splenocytes were cultured with concanavalin A for 24 h at 37 °C in 5% CO_2. Following washing, 4×10^4 splenocytes were incubated with 3 ng/mL IL-2 and test compounds at designated concentrations in 96-well tissue culture plates. After incubation for 72 h, alamarBlue® (Life Technologies, Carlsbad, CA, USA) was added to each of the test wells, followed by incubation for 6 h. Fluorescence intensity was measured at an excitation wavelength of 545 nm and an emission wavelength of 590 nm. Duplicate experiments were conducted for test compounds, and the IC_{50} value of each experiment was calculated using linear regression analysis.

4.2.5. Rat adjuvant-induced arthritis (AIA) model.

The adjuvant-induced arthritis (AIA) model shares a number of pathologic, genetic, and immunologic features with RA. Therefore, the AIA rat model was used to evaluate the effects of oral **13t** (50, 100 mg/kg p.o.) on joint inflammation and histopathology. Arthritis was induced by immunization of male Lewis rats (8 to 10 weeks old) via intradermal injection at the base of the toe with complete Freund's adjuvant with three 50 μL injections (10 mg/mL Mycobacterium tuberculosis in incomplete Freund's adjuvant (Sigma Aldrich)). When individual hind paw volume measurements indicated an increase of 0.2 mL (or greater) in a single hind paw, animals were randomly assigned to a treatment group. On the day treatment was initiated, the rats were randomly assigned to controls (no adjuvant injection plus vehicle; n = 6), injection plus vehicle (n = 6), injection plus **13t** 50 mg/kg (n = 6), injection plus **13t** 100 mg/kg (n = 6) and injection plus tofacitinib 25 mg/kg (n = 6). The rats were monitored three days per time for signs of arthritis including change in body weight and hind paw volume measurement. On day 35 all animals were euthanized, samples for clinical chemistry and hematology were collected, and hind limbs were removed and placed in 10% formalin for computed tomography (CT) imaging and histologic analysis.

4.3. Docking calculation

The crystal structure of the JAK3 kinase domain was obtained from the Protein Data Bank (PDB code 4Z16) [15]. Water molecules were removed, and hydrogen atoms were added to the structure. Three dimensional structure of the compounds were generated and optimized by the Discovery Studio 3.0 package. The small molecule was docked into the JAK3 domain using the Covalent Dock Cloud server (http://docking.sce.ntu.edu.sg) [32]. The top-scoring pose was employed for discussions.

Declaration of Competing Interest

The authors declare that they have no known competing financial interests or personal relationships that could have appeared to influence the work reported in this paper.

Acknowledgements

The authors are grateful to financial supports from the National Natural Science Foundation of China (81573445, 81172934, 81973338), and Beijing Municipal Natural Science Foundation (7182115).

Declaration of Competing Interest

The authors have declared no conflict of interest.

Appendix A. Supplementary material

Supplementary data to this article can be found online at https://doi.org/10.1016/j.bioorg.2020.103720.

References

[1] C.M. Weyand, J.J. Goronzy, S. Takemura, P.J. Kurtin, Cell-cell interactions in

synovitis: Interactions between T cells and B cells in rheumatoid arthritis, Arthritis Res. Therapy 2 (2000) 374.
[2] J.S. Smolen, D. Aletaha, I.B. Mclnnes, Rheumatoid arthritis, Lancet 388 (2016) 2023–2038.
[3] I.B. McInnes, G. Schett, The pathogenesis of rheumatoid arthritis, New. Engl. J. Med 365 (2011) 2205–2219.
[4] D.M. Schwartz, M. Bonelli, M. Gadina, J.J. O'Shea, Type I/II cytokines, JAKs, and new strategies for treating autoimmune diseases, Nat. Rev. Rheumatol 12 (2016) 25–36.
[5] H. Wang, J. Brown, S. Gao, S. Liang, R. Jotwani, H. Zhou, J. Suttles, D. Scott, R.J. Lamont, The role of JAK-3 in regulating TLR-mediated inflammatory cytokine production in innate immune cells, J. Immunol 191 (2013) 1164–1174.
[6] K. Ghoreschi, A. Laurence, J.J. O'Shea, Janus kinases in immune cell signaling, Immunol. Rev 228 (2009) 273–287.
[7] A. Laurence, M. Pesu, O. Silvennoinen, J. O'Shea, Suppl 2: JAK Kinases in Health and Disease: An Update, Open. Rheumatol. J 6 (2012) 232–244.
[8] T. Musso, J.A. Johnston, D. Linnekin, L. Varesio, T.K. Rowe, J.J. O'Shea, D.W. McVicar, Regulation of JAK3 expression in human monocytes: phosphorylation in response to interleukins 2, 4, and 7, J. Exp. Med 181 (1995) 1425–1431.
[9] M. Kawamura, D.W. McVicar, J.A. Johnston, T.B. Blakeo, Y.Q. Chen, B.K. Lal, A.R. Lloyd, D.J. Kelvin, J.E. Staples, J.R. Ortaldo, J.J. O'Shea, Molecular cloning of L-JAK, a Janus family protein-tyrosine kinase expressed in natural killer cells and activated leukocytes, P. Natl. A. Sci 91 (1994) 6374–6378.
[10] J.J. O'Shea, D.M. Schwartz, A.V. Villarino, M. Gadina, I.B. McInnes, A. Laurence, The JAK-STAT pathway: impact on human disease and therapeutic intervention, Annu. Rev. Med 66 (2015) 311–328.
[11] J.J. O'Shea, R. Plenge, JAK and STAT signaling molecules in immunoregulation and immune-mediated disease, Immunity 36 (2012) 542–550.
[12] P.S. Changelian, M.E. Flanagan, D.J. Ball, C.R. Kent, Prevention of organ allograft rejection by a specific Janus kinase 3 inhibitor, Science 302 (2003) 875–878.
[13] D. Vyas, K.M. O'Dell, J.L. Bandy, E.G. Boyce, Tofacitinib: The First Janus Kinase (JAK) inhibitor for the treatment of rheumatoid arthritis, Ann. Pharmacother 47 (2013) 1524–1531.
[14] K.L. Winthrop, The emerging safety profile of JAK inhibitors in rheumatic disease, Nat. Rev. Rheumatol 13 (2017) 234–243.
[15] L. Tan, K. Akahane, R. McNally, K.M.S. Reyskens, S.B. Ficarro, Development of selective covalent Janus kinase 3 inhibitors, J. Med. Chem 58 (2015) 6589–6606.
[16] G. Thoma, P. Drückes, H.G. Zerwes, Selective inhibitors of the Janus kinase Jak3-Are they effective? Bioorg. Med. Chem. Lett 24 (2014) 4617–4621.
[17] M.C. Genovese, R.V. Vollenhoven, B.J. Bloom, J.G. Jiang, N. Kinnman, A phase 2b, 12-week study of VX-509, an oral selective Janus kinase 3 inhibitor, in combination with background methotrexate in rheumatoid arthritis, Arthritis. Rheumatol 65 (2013) 3320.
[18] Q. Liu, Y. Sabnis, Z. Zhao, T. Zhang, S.J. Buhrlage, L.H. Jones, N.S. Gray, Developing irreversible inhibitors of the protein kinase cysteinome, Chem. Biol 20 (2013) 146–159.
[19] D. Li, L. Ambrogio, T. Shimamura, S. Kubo, M. Takahashi, L.R. Chirieac, R.F. Padera, G.I. Shapiro, A. Baum, F. Himmelsbach, W.J. Rettig, M. Meyerson, F. Solca, H. Greulich, K.K. Wong, BIBW2992, an irreversible EGFR/HER2 inhibitor highly effective in preclinical lung cancer models, Oncogene 27 (2008) 4702–4711.
[20] J.R. Brown, Ibrutinib (PCI-32765), the first BTK (Bruton's tyrosine kinase) inhibitor in clinical trials, Curr. Hematol, Malig. R 8 (2013) 1–6.
[21] W. Zhou, D. Ercan, L. Chen, C.H. Yun, D. Li, M. Capelletti, A.B. Cortot, L. Chirieac, R.E. Iacob, R. Padera, J.R. Engen, K.K. Wong, M.J. Eck, N.S. Gray, P.A. Janne, Novel mutantselective EGFR kinase inhibitors against EGFR T790M, Nature 462 (2009) 1070–1074.
[22] J.B. Telliez, M.E. Dowty, L.U. Wang, J. Jussif, T. Lin, L. Li, Discovery of a JAK3-selective inhibitor: functional differentiation of JAK3-selective inhibition over pan-JAK or JAK1-selective inhibition, ACS. Chem. Biol 11 (2016) 3442–3451.
[23] M. Forster, A. Chaikuad, S.M. Bauer, J. Holstein, M.B. Robers, C.R. Corona, M. Gehringer, E. Pfaffenrot, K. Ghoreschi, S. Knapp, S.A. Laufer, Selective JAK3 Inhibitors with a Covalent Reversible Binding Mode Targeting a New Induced Fit Binding Pocket, Cell. Chem. Biol 23 (2016) 1335–1340.
[24] G.A. Smith, K. Uchida, A. Weiss, J. Taunton, Essential biphasic role for JAK3 catalytic activity in IL-2 receptor signaling, Nat. Chem. Biol 12 (2016) 373–379.
[25] Y. Yin, C.J. Chen, R.N. Yu, Z.J. Wang, T.T. Zhang, D.Y. Zhang, Structure-Based Design and Synthesis of 1*H*-pyrazolo[3, 4-*d*]pyrimidin-4-amino Derivatives as Janus Kinase 3 Inhibitors, Bioorg. Med. Chem 26 (2018) 4774–4786.
[26] N. Ramsden, R. J. Harrison, S. Oxenford, K. Bell, N. Piton, C. Dagostin, C. Boussard, A. Ratcliffe, Heterocyclyl pyrazolopyrimidine analogues as JAK inhibitors, WO2011048082A1.
[27] S. Li, X. Cheng, Y. Zhou, Z. Xi, Sparsomycin-Linezolid Conjugates Can Promote Ribosomal Translocation, Chembiochem 12 (2011) 2801–2806.
[28] F. Yuan, X.J. Chen, Y.H. Zhou, F. Yang, Q.L. Zhang, J. Liu, Synthesis of a ruthenium (II) polypyridine complex with 1, 10-phenanthrolineselenazole as ligand and investigation of its G-quadruplex DNA-binding properties, J. Coord. Chem 65 (2012) 1246–1257.
[29] S. Babu, C. Morrill, N.G. Almstead, Y.C. Moon, Selective synthesis of 1-substituted 4-chloropyrazolo[3, 4-*d*]pyrimidines, Org. Lett 15 (2013) 1882–1885.
[30] F. Elwood, D.J. Witter, J. Piesvaux, B. Kraybill, N. Bays, C. Alpert, P. Goldenblatt, Y.J. Qu, Evaluation of JAK3 biology in autoimmune disease using a highly selective, irreversible JAK3 inhibitor, J. Pharmacol. Exp. Ther 361 (2017) 229–244.
[31] T. Barf, A. Kaptein, Irreversible protein kinase inhibitors: balancing the benefits and risks, J. Med. Chem 55 (2012) 6243–6262.
[32] X. Ouyang, S. Zhou, C.T.T. Su, Z. Ge, R. Li, C.K. Kwoh, Covalent dock: automated covalent docking with parameterized covalent linkage energy estimation and molecular geometry constrains, J. Comput. Chem. 34 (2013) 326–336.